Research Square

Preprints are preliminary reports that have not undergone peer review.
They should not be considered conclusive, used to inform clinical practice,
or referenced by the media as validated information.

Design, synthesis, characterization and biomimetic evaluation of novel chrysin derivatives of copper(II) complexes as medicinal purpose

Ebenezer Bonpandi (ebichem@gmail.com)
Manonmaniam Sundaranar University
Nagashri Kandasamy
Manonmaniam Sundaranar University

Research Article

Keywords: Copper complexes, Biomimetic, Antimicrobial, Anti-proliferative, Anti-inflammatory, Cholinesterase activity

Posted Date: August 3rd, 2022

DOI: https://doi.org/10.21203/rs.3.rs-1881912/v1

License: This work is licensed under a Creative Commons Attribution 4.0 International License. Read Full License

Abstract

Background

In the present investigations, a novel series of chrysin (5,7-dihydroxyflavone) derivatives were prepared using Mannich base approach. Copper complexes of molecular formulae, [Cu-L(OAc)(H_2O)] where Cu-a to Cu-h represents Schiff base ligands [by the condensation of chrysin with aliphatic / aromatic / heterocyclic amines], have been prepared.

Methods

Synthesis copper complexes were characterized using analytical and spectral techniques. The *in vitro* antimicrobial activities of the synthesized compounds were tested against the bacterial species and fungal species. Antioxidant activities and SOD effect of the copper complexes have also been studied. The DNA binding and DNA cleavage activity of copper complexes were studied. The screened for *in vitro* anti-proliferative activity against human cancer cells (HeLa and MCF-7). The effective complexes was subjected to anti-mycobacterial activity using MABA method and summarized. The Cholinesterase inhibitory activity (AChE and BuChE) of ligand was screened using modified Ellman's method. The α-glucosidase inhibition activity was also carried out for the prepared copper complexex. In addition, CAT activity and lipophilic behaviour were also assessed.

Conclusion

The prepared compound exhibited strong anti-proliferative efficacies may be mimics the natural chrysin derivatives. The utmost promising structural lead molecules in particular the chrysin derivatives Cu-g and Cu-h, will be screened for their anti-proliferative activities against a broader range of cancer cell lines and may be potent molecule for anticancer agents.

Highlights

- A novel series of chrysin derivatives were prepared using Mannich base approach. Copper complexes of Schiff base ligands have been prepared.
- *In vitro* antimicrobial activities of the synthesized compounds were tested against the bacterial species and fungal species.
- Antioxidant activities and SOD effect of the copper complexes have also been studied.
- DNA binding and DNA cleavage activity has also been studied.
- The screened for *in vitro* anti-proliferative activity against human cancer cells (HeLa and MCF-7).
- Anti-tuberculosis activity was also performed using MABA method and summarized.
- The lipophilicity of copper complexes was measured using the shake flask method.
- The prepared copper complexes were accessed cholinesterase and α-Glucosidase inhibitory activities.

Introduction

Platinum-based drugs such as cisplatin are powerful anticancer agents. But they have undesirable side effects and are effective against only a few kinds of cancers. Therefore, there is a need for new metal based drugs with an improved spectrum of efficacy and lower toxicity. Therefore, synthetic chemists search for new, less toxic, more effective and preventive drugs based on copper complexes for the treatment of Cervical Cancer. Natural phytoconstituents and their chemically modified derivatives provide a diverse set of unique chemical entities for use in medication development for a variety of clinical cancer cell lines [1–4].

According to the literature, pharmacological screening of natural compounds has a wide range of clinical uses for a variety of problems. Flavonoids are natural phytochemicals and secondary metabolites generated from plants that are abundant in fruits and vegetables [5]. Flavonoids are well-known for their wide variety of health benefits, particularly in the prevention of secondary problems and the reduction of oxidative stress [6]. One or more ortho hydroxyl phenolic groups are present in flavonoids, as well as one phenolic group with an adjacent carbonyl group. Due to the presence of an α-hydroxycarbonyl group, flavonol is known to have a high affinity for chelating metal ions among the flavonoids [7]. Favonoids or favonoid derivatives appear to play an important role in cancer chemoprevention and chemotherapy, according to a growing number of studies. A number of epidemiological studies suggest that greater favonoid intake is linked to a lower incidence of cancer, indicating that favonoids may have a preventive role in cancer prevention [8, 9]. *In vitro* studies suggest that favonoids anticancer properties are linked to reducing cell proliferation, adhesion and invasion, as well as causing cell differentiation, cell cycle arrest and death, among other things [10, 11].

Chrysin (5,7-dihydroxyflavone) is a flavone derivative found in a variety of plant species, fruits, and vegetables. Many biological activities were found in the literature resources, including anticancer, antiviral, antibacterial, antiallergic, antimutagenic, antianxiolytic, anti-inflammatory, and so on. Many researchers from all around the world have recently modified the structural core of chrysin with other chemical compounds, resulting in a wide range of biological actions. Many study groups have been inspired by the organic transformation reactions of naturally generated chemicals, which include oxidation, reduction, Schiff base, mannich base, cyclization, dehydration and other transformations [12–16].

After iron and zinc, copper is the body's third most prevalent element. It's found in everything from microbes to mammals, and it's essential to their survival. Copper complexes are key bioactive molecules *in vitro* and *in vivo* and their use as possible medicines for a variety of ailments is growing in popularity. Copper synthetic compounds can accelerate nucleic acid (particularly DNA) cleavage, thus they're worth testing against cancer cells both *in vitro* and *in vivo* [17]. Metal-based medications have been thrust into the forefront of the fight against cancer as a result of the development of medical inorganic chemistry, particularly the discovery of cisplatin's anticancer properties. Coppers homeostasis and metabolism are vital for all types of human malignancies, and copper levels in cancer patients' tumour tissue are much higher than normal tissue. As a result, cancer cells could be a good target for copper-based medicines Copper also changes the metabolism of cancer cells and has a different reaction to tumour cells than normal cells, giving copper complexes important anti-cancer properties. As a result, copper complexes have shown promising results and are being evaluated as potential platinum medication substitutes [18–20]. Many studies have demonstrated that copper complexes play a key role in the endogenous oxidative DNA damage linked to ageing and cancer in recent years. As a result, copper complex production and biological testing have become key topics of current research [21]. Copper is an essential trace metal for plants and animals, and it plays a role in the production of mixed ligand complexes in a variety of biological processes. Copper (II) complexes containing Schiff base ligands are of particular relevance because they have anticancer properties. As a result, they can be utilized as chemical nucleases and chemotherapeutic treatments for cancer [22].

In the present work was concentrated on the preparation of different copper complexes and chrysin derivatives using Mannich base and Schiff base approach (Scheme 1). They were characterized using analytical and spectral techniques. Furthermore, their biological studies like anti-microbial activity, anti-oxidant, SOD activity, DNA binding and cleavage activity, anti-proliferative activity, anti-inflammatory. They were structurally elucidated and screened for and anti-proliferative potency against cell lines (HeLa and MCF-7) with the help of MTT assay. The synthesized compounds were evaluated by AChE/BuChE inhibitory activity.

Experimental

Materials and methods

All chemicals, reagents and solvents used in this work were bought from Sigma. Thin Layer Chromatography (TLC) was used to monitor the reactions progress using prepared, silica gel-coated plates. Purification was achieved using column chromatography with the appropriate mesh and size (60–120) of silica gel. An Elemental Analyzer Carlo Erba EA1108 was

used to record the C, H, N composition analyses. Copper was measured using a gravimetric approach, utilizing cuprous thiocyanate, respectively. A Shimadzu FT-IR Affinity-1 spectrophotometer was used to record FT-IR spectra of ligands and their copper complexes. A Systronics UV–visible spectrophotometer (200–1000 nm) was used to record the electronic absorption spectra of chrysin derivatives and copper complexes. Using a BRUKER 400 MHz spectrometer and the ^{1}H NMR spectra of the ligand, the type of proton and anionic coordination sites was determined. Chemical changes are expressed in parts per million (ppm) in comparison to TMS (tetramethylsilane), which serves as an internal reference. Using a JEOL SX 102/DA-6000 mass spectrometer/data system, the Fast Atom Bombardment (FAB) mass spectra demonstrate the molecular mass and fragmentation of ligands and copper complexes. The molar conductance was measured using the Systronics conductivity bridge and the magnetic moment was estimated using Guoy's electronic balance. The electrochemical properties of copper complexes were investigated using a three-electrode cell assembly with platinum electrode as working electrode, standard calomel as reference electrode and platinum as auxiliary electrode in DMSO (dimethyl sulfoxide) ($n\text{-}Bu_4NClO_4$ as supporting electrolyte). Using Perkin Elmer equipment, thermal studies of complexes were carried out under nitrogen at a heating rate of 10 °C min^{-1}.

Preparation of chrysin derivatives

In the first stage, the chrysin (0.01 mM) and appropriate amount of toluene (20 mL) was taken in a RB flask. After complete solubility of chrysin, n-methylmorpholine (1.0 mL) and a drop of n-propyl amine / n-pentyl amine (0.01 mM) was slowly added into the solution. Then, the reaction mixture was manually stirred for 3 hrs at 50 ℃. It was allowed to cool at RT and stand overnight. Then, a yellow solid was filtered with the thoroughly washing with water (15 mL) and diethyl ether (15 mL) and dried under vacuum. In the second stage, the 0.001 M of above product was mixed with paraformaldehyde (0.001 M) were mixed in hot ethanol (2 mL). The different primary amine (0.001 M) was slowly added into the reaction. Then, the reaction mixture was stirred about 4 hrs at RT. The different coloured solids were separated with the help of filtering, washing with ethyl acetate & ether and dried under vacuum (Scheme 1).

Synthesis of 5,7-dihydroxy-2-phenyl-1-propyl-8-((propylamino)methyl)quinolin-4(1H)-one **(3a):** Mol. Formula: $C_{22}H_{26}N_2O_3$. MW = 566. Yield: 81%. CHN: Anal. calcd for: C, 72.11; H, 7.15; N, 7.64. Found: C, 71.32; H, 6.41; N, 7.57. Fast atom bombardment mass spectrometry (FAB-MS), *m/z* 367 [M+1]. ^{1}H NMR (400 MHz, $CDCl_3$, δ, ppm): 6.57 (1H, s, -CH), 6.9 (1H, s, -CH), 7.12-7.36 (5H, m, Ar-H, -CH), 3.07 (2H, t, $-CH_2$), 1.56 (2H, m, $-CH_2$), 0.97 (3H, t, $-CH_3$), 3.83 (2H, s, $-CH_2$), 2.05 (1H, -NH), 2.58 (2H, m, -CH), 1.48 (2H, m, $-CH_2$), 0.98 (3H, t, $-CH_3$) 10.96 (1H, s, D_2O exchange, -OH), 10.22 (1H, s, D_2O exchange, -OH). ^{13}C NMR (400 MHz, $CDCl_3$, ppm): 162.2 (C_2), 97.2 (C_3), 182.2 (C_4), 162.4 (C_5), 92.3 (C_6), 163.6 (C_7), 101.3 (C_8), 145.5 (C_9), 111.7 (C_{10}), 134.3 (C_{11}), 126.4 ($C_{12,16}$), 128.6 ($C_{13,15}$), 128.1 (C_{14}), 46.8 (C_{17}), 21.7 (C_{18}), 11.9 (C_{19}), 36.3 (C_{20}), 51.8 (C_{22}), 23.9 (C_{23}), 11.6 (C_{24}).

Synthesis of 8-((diethylamino)methyl)-5,7-dihydroxy-2-phenyl-1-propylquinolin-4(1H)-one **(3b):** Mol. Formula: $C_{23}H_{28}N_2O_3$. MW = 380. Yield: 67%. CHN: Anal. calcd for: C, 72.60; H, 7.42; N, 7.36. Found: C, 72.02; H, 7.09; N, 7.51. Fast atom bombardment mass spectrometry (FAB-MS), *m/z* 381 [M+1]. ^{1}H NMR (400 MHz, $CDCl_3$, δ, ppm): 6.57 (1H, s, -CH), 7.0 (1H, s, -CH), 7.12-7.36 (5H, m, Ar-H, -CH), 3.07 (2H, t, $-CH_2$), 1.56 (2H, m, $-CH_2$), 0.97 (3H, t, $-CH_3$), 3.65 (2H, s, $-CH_2$), 2.43 (4H, m, $-CH_2$), 1.03 (6H, t, $-CH_3$), 10.93 (1H, s, D_2O exchange, -OH), 10.16 (1H, s, D_2O exchange, -OH). ^{13}C NMR (400 MHz, $CDCl_3$, ppm): 162.3 (C_2), 97.2 (C_3), 182.1 (C_4), 162.4 (C_5), 92.5 (C_6), 164.4 (C_7), 100.2 (C_8), 146.6 (C_9), 111.7 (C_{10}), 134.2 (C_{11}), 126.5 ($C_{12,16}$), 128.6 ($C_{13,15}$), 128.1 (C_{14}), 46.7 (C_{17}), 21.7 (C_{18}), 11.8 (C_{19}), 41.9 (C_{20}), 49.4 (C_{22} - C_{24}), 13.7 (C_{23} - C_{25}).

Synthesis of 8-((1H-pyrrol-1-yl)methyl)-5,7-dihydroxy-2-penyl-1-propylquinolin-4(1H)-one **(3c):** Mol. Formula: $C_{23}H_{22}N_2O_3$. MW = 374. Yield: 71%. CHN: Anal. calcd for: C, 73.78 ; H, 5.92; N, 7.48. Found: C, 73.13; H, 5.32; N, 7.51. Fast atom bombardment mass spectrometry (FAB-MS), *m/z* 375 [M+1]. ^{1}H NMR (400 MHz, $CDCl_3$, δ, ppm): 6.57 (1H, s, -CH), 7.1 (1H, s, -CH), 7.12-7.36 (5H, m, Ar-H, -CH), 3.07 (2H, t, $-CH_2$), 1.56 (2H, m, $-CH_2$), 0.96 (3H, t, $-CH_3$), 5.12 (2H, s, $-CH_2$), 6.00 – 6.53 (4H, m, -CH), 10.87 (1H, s, D_2O exchange, -OH), 10.18 (1H, s, D_2O exchange, -OH). ^{13}C NMR (400 MHz, $CDCl_3$, ppm): 162.3 (C_2), 97.1 (C_3), 182.4 (C_4), 161.5 (C_5), 92.2 (C_6), 164.5 (C_7), 101.7 (C_8), 146.7 (C_9), 111.5 (C_{10}), 134.3 (C_{11}), 126.4 ($C_{12,16}$), 128.6 ($C_{13,15}$), 128.1 (C_{14}), 46.9 (C_{17}), 21.8 (C_{18}), 11.8 (C_{19}), 38.6 (C_{20}), 122.7 (C_{22} - C_{24}), 108.8 (C_{23} - C_{25}).

Synthesis of 8-(N-ethyl-N-phenylamino)-5,7-dihydroxy-2-phenyl-1-propylquinolin-4(1H)-one **(3d):** Mol. Formula: $C_{27}H_{28}N_2O_3$. MW = 428. Yield: 67%. CHN: Anal. calcd for: C, 75.34 ; H, 6.32; N, 6.76. Found: C, 75.13; H, 6.18; N, 6.59. Fast atom bombardment mass spectrometry (FAB-MS), *m/z* 429 [M+1]. ^{1}H NMR (400 MHz, $CDCl_3$, δ, ppm): 6.57 (1H, s, -CH), 7.1 (1H, s, -CH), 7.12-7.36 (5H, m, Ar-H, -CH), 3.07 (2H, t, $-CH_2$), 1.57 (2H, m, $-CH_2$), 0.97 (3H, t, $-CH_3$), 4.64 (2H, s, $-CH_2$), 6.55 – 7.10 (6H, m, -CH), 3.37 (2H, t, $-CH_2$), 1.16 (3H, s, $-CH_3$), 11.13 (1H, s, D_2O exchange, -OH), 10.23 (1H, s, D_2O exchange, -OH). ^{13}C NMR (400 MHz, $CDCl_3$, ppm): 162.2 (C_2), 97.2 (C_3), 182.2 (C_4), 162.4 (C_5), 92.2 (C_6), 163.3 (C_7), 101.4 (C_8), 145.5 (C_9), 111.7 (C_{10}), 134.3 (C_{11}), 126.4 ($C_{12,16}$), 128.6 ($C_{13,15}$), 128.3 (C_{14}), 46.9 (C_{17}), 21.6 (C_{18}), 11.6 (C_{19}), 34.8 (C_{20}), 149.7 (C_{22}), 114.5 (C_{23} - C_{27}), 129.7 (C_{24} - C_{26}), 118.6 (C_{25}), 44.7 (C_{28}), 13.4 (C_{29}).

Synthesis of 5,7–dihydroxy-1-pentyl-2-phenyl-8-((propylamino)methyl)quinolin-4(1H)-one **(3e):** Mol. Formula: $C_{24}H_{30}N_2O_3$. . MW = 394. Yield: 77%. CHN: Anal. calcd for: C, 73.07 ; H, 7.66; N, 7.10. Found: C, 72.41; H, 7.29; N, 7.26. Fast atom bombardment mass spectrometry (FAB-MS), *m/z* 395 [M+1]. ^{1}H NMR (400 MHz, $CDCl_3$, δ, ppm): 6.58 (1H, s, -CH), 7.1 (1H, s, -CH), 7.12-7.36 (5H, m, Ar-H, -CH), 3.02 (2H, t, $-CH_2$), 1.56 (2H, m, $-CH_2$), 1.29 (2H, m, $-CH_2$), 1.35 (2H, m, $-CH_2$), 0.95 (3H, t, $-CH_3$), 3.81 (2H, s, $-CH_2$), 2.03 (1H, -NH), 2.56 (2H, m, -CH), 1.49 (2H, m, $-CH_2$), 0.97 (3H, t, $-CH_3$), 10.98 (1H, s, D_2O exchange, -OH), 10.11 (1H, s, D_2O exchange, -OH). ^{13}C NMR (400 MHz, $CDCl_3$, ppm): 162.4 (C_2), 97.1 (C_3), 182.3 (C_4), 162.5 (C_5), 92.1 (C_6), 163.3 (C_7), 101.6 (C_8), 145.4 (C_9), 111.7 (C_{10}), 134.1 (C_{11}), 126.2 ($C_{12,16}$), 128.9 ($C_{13,15}$), 127.8 (C_{14}), 44.2 (C_{17}), 28.1 (C_{18}), 29.9 (C_{19}), 22.8 (C_{20}), 14.2 (C_{21}), 36.5 (C_{22}), 51.8 (C_{24}), 23.9 (C_{25}), 11.6 (C_{26}).

Synthesis of 8-((diethylamino)methyl)-5,7–dihydroxy-1-pentyl-2-phenyl-quinolin-4(1H)-one **(3f):** Mol. Formula: $C_{25}H_{32}N_2O_3$. MW = 408. Yield: 71%. CHN: Anal. calcd for: C, 73.50 ; H, 7.90; N, 6.86. Found: C, 72.89; H, 7.44; N, 7.01. Fast atom bombardment mass spectrometry (FAB-MS), *m/z* 409 [M+1]. ^{1}H NMR (400 MHz, $CDCl_3$, δ, ppm): 6.59 (1H, s, -CH), 7.2 (1H, s, -CH), 7.12-7.36 (5H, m, Ar-H, -CH), 3.04 (2H, t, $-CH_2$), 1.59 (2H, m, $-CH_2$), 1.26 (2H, m, $-CH_2$), 1.34 (2H, m, $-CH_2$), 0.97 (3H, t, $-CH_3$), 3.67 (2H, s, $-CH_2$), 2.44 (4H, m, $-CH_2$), 1.06 (6H, t, $-CH_3$), 10.89 (1H, s, D_2O exchange, -OH), 10.24 (1H, s, D_2O exchange, -OH). ^{13}C NMR (400 MHz, $CDCl_3$, ppm): 162.5 (C_2), 97.4 (C_3), 182.1 (C_4), 162.1 (C_5), 92.5 (C_6), 164.1 (C_7), 100.1 (C_8), 146.7 (C_9), 111.5 (C_{10}), 134.5 (C_{11}), 126.6 ($C_{12,16}$), 128.8 ($C_{13,15}$), 128.3 (C_{14}), 44.7 (C_{17}), 28.5 (C_{18}), 29.6 (C_{19}), 22.4 (C_{20}), 14.3 (C_{21}), 41.6 (C_{22}), 49.6 (C_{24} - C_{26}), 13.5 (C_{25} - C_{27}).

Synthesis of 8-((1H-pyrrol-1-yl)methyl)-5,7-dihydroxy-1-pentyl-2-phenyl-quinolin-4(1H)-one **(3g):** Mol. Formula: $C_{25}H_{26}N_2O_3$. MW = 402. Yield: 69%. CHN: Anal. calcd for: C, 74.60 ; H, 6.51; N, 6.96. Found: C, 74.09; H, 6.14; N, 7.13. Fast atom bombardment mass spectrometry (FAB-MS), *m/z* 403 [M+1]. ^{1}H NMR (400 MHz, $CDCl_3$, δ, ppm): 6.57 (1H, s, -CH), 7.1 (1H, s, -CH), 7.12-7.36 (5H, m, Ar-H, -CH), 3.06 (2H, t, $-CH_2$), 1.55 (2H, m, $-CH_2$), 1.29 (2H, m, $-CH_2$), 1.31 (2H, m, $-CH_2$), 0.94 (3H, t, $-CH_3$), 5.11 (2H, s, $-CH_2$), 6.00-6.53 (4H, m, -CH), 10.98 (1H, s, D_2O exchange, -OH), 10.51 (1H, s, D_2O exchange, -OH). ^{13}C NMR (400 MHz, $CDCl_3$, ppm): 162.1 (C_2), 97.3 (C_3), 182.1 (C_4), 161.4 (C_5), 92.1 (C_6), 164.5 (C_7), 101.5 (C_8), 146.6 (C_9), 111.6 (C_{10}), 134.1 (C_{11}), 126.6 ($C_{12,16}$), 128.9 ($C_{13,15}$), 128.0 (C_{14}), 44.5 (C_{17}), 28.1 (C_{18}), 29.5 (C_{19}), 22.6 (C_{20}), 14.4 (C_{21}),38.8 (C_{22}), 122.6 (C_{24} - C_{26}), 108.6 (C_{25} - C_{27}).

Synthesis of 8-((N-ethyl-N-phenylamino)methyl)-5,7-dihydroxy-1-pentyl-2-phenylquinolin-4(1H)-one **(3h):** Mol. Formula: $C_{29}H_{32}N_2O_3$. MW = 456. CHN: Yield: 72%. Anal. calcd for: C, 76.29 ; H, 6.83; N, 6.14. Found: C, 75.82; H, 6.67; N, 6.21. Fast atom bombardment mass spectrometry (FAB-MS), *m/z* 457 [M+1]. ^{1}H NMR (400 MHz, $CDCl_3$, δ, ppm): 6.58 (1H, s, -CH), 7.1 (1H, s, -CH), 7.12-7.36 (5H, m, Ar-H, -CH), 3.06 (2H, t, $-CH_2$), 1.56 (2H, m, $-CH_2$), 1.29 (2H, m, $-CH_2$), 1.36 (2H, m, $-CH_2$), 0.94 (3H, t, $-CH_3$), 4.65 (2H, s, $-CH_2$), 6.55 – 7.10 (6H, m, -CH), 3.36 (2H, t, $-CH_2$), 1.17 (3H, s, $-CH_3$), 10.92 (1H, s, D_2O exchange, -OH), 10.23 (1H, s, D_2O exchange, -OH). ^{13}C NMR (400 MHz, $CDCl_3$, ppm): 162.4 (C_2), 97.0 (C_3), 182.1 (C_4), 162.4 (C_5), 92.5 (C_6), 163.1 (C_7), 101.1 (C_8), 145.3 (C_9), 111.5 (C_{10}), 134.5 (C_{11}), 126.2 ($C_{12,16}$), 128.5 ($C_{13,15}$), 128.3 (C_{14}), 44.1 (C_{17}), 28.5 (C_{18}), 29.9 (C_{19}), 22.9 (C_{20}), 14.3 (C_{21}), 34.6 (C_{22}), 149.8 (C_{24}), 114.9 (C_{25} - C_{29}), 129.8 (C_{26} - C_{28}), 118.7 (C_{27}), 44.8 (C_{30}), 13.1 (C_{31}).

Synthesis of Copper Complexes of Ligands

In hot ethanol (20 mL), ligand (0.05 mM) and copper acetate (0.05 mM) have been dissolved. The triethylamine (0.075 mM) was then dropped cautiously to the mixture under stirring. Heat up the solution in string condition for 5 hrs, then pour it into the water. The precipitate obtained was dissolved in DMC (dichloromethane), washed with water, dried over sodium sulphate and purified by column chromatography in chloroform: methanol medium.

Copper Complex of Cu-a: Mol. Formula: $C_{24}H_{30}CuN_2O_7$. MW = 506. Yield: 74%. Anal. Calcd for $C_{24}H_{30}CuN_2O_6$: C, 56.96; H, 5.98; Cu, 12.56; N, 5.54. Found: C, 56.82; H, 5.88; Cu, 12.41; N, 5.43. FAB mass spectrometry (FAB-MS): m/z 507 [M+1]. μ_{eff} (BM) = 1.72; Δm (mhocm^2 mol^{-1}) = 20.

Copper Complex of Cu-b: Mol. Formula: $C_{25}H_{32}CuN_2O_7$. MW = 520. Yield: 78%. Anal. Calcd for $C_{25}H_{32}CuN_2O_6$: C, 57.74; H, 6.20; Cu, 12.22; N, 5.39. Found: C, 57.65; H, 6.08; Cu, 12.12; N, 5.22. FAB mass spectrometry (FAB-MS): m/z 521 [M+1]. μ_{eff} (BM) = 1.93; Δm (mhocm^2 mol^{-1}) = 22.

Copper Complex of Cu-c: Mol. Formula: $C_{25}H_{26}CuN_2O_7$. MW = 514. Yield: 81%. Anal. Calcd for $C_{25}H_{26}CuN_2O_6$: C, 58.41; H, 5.10; Cu, 12.36; N, 5.45. Found: C, 58.31; H, 5.03; Cu, 12.25; N, 5.32. FAB mass spectrometry (FAB-MS): m/z 515 [M+1]. μ_{eff} (BM) = 1.94; Δm (mhocm^2 mol^{-1}) = 19.

Copper Complex of Cu-d: Mol. Formula: $C_{29}H_{32}CuN_2O_7$. MW = 568. Yield: 75%. Anal. Calcd for $C_{29}H_{32}CuN_2O_6$: C, 61.31; H, 5.68; Cu, 11.19; N, 4.93. Found: C, 61.23; H, 5.60; Cu, 11.04; N, 4.79. FAB mass spectrometry (FAB-MS): m/z 569 [M+1]. μ_{eff} (BM) = 1.92; Δm (mhocm^2 mol^{-1}) = 18.

Copper Complex of Cu-e: Mol. Formula: $C_{26}H_{34}CuN_2O_7$. MW = 534. Yield: 74%. Anal. Calcd for $C_{26}H_{34}CuN_2O_6$: C, 58.47; H, 6.42; Cu, 11.90; N, 5.24. Found: C, 58.32; H, 6.31; Cu, 11.76; N, 5.11. FAB mass spectrometry (FAB-MS): m/z 535 [M+1]. μ_{eff} (BM) = 1.88; Δm (mhocm^2 mol^{-1}) = 20.

Copper Complex of Cu-f: Mol. Formula: $C_{27}H_{36}CuN_2O_7$. MW = 548. Yield: 78%. Anal. Calcd for $C_{27}H_{36}CuN_2O_6$: C, 59.16; H, 6.62; Cu, 11.59; N, 5.11. Found: C, 59.04; H, 6.53; Cu, 11.47; N, 5.03. FAB mass spectrometry (FAB-MS): m/z 549 [M+1]. μ_{eff} (BM) = 1.98; Δm (mhocm^2 mol^{-1}) = 22.

Copper Complex of Cu-g: Mol. Formula: $C_{27}H_{30}CuN_2O_7$. MW = 542. Yield: 81%. Anal. Calcd for $C_{27}H_{30}CuN_2O_6$: C, 59.82; H, 5.58; Cu, 11.72; N, 5.17. Found: C, 59.72; H, 5.49; Cu, 11.58; N, 5.02. FAB mass spectrometry (FAB-MS): m/z 543 [M+1]. μ_{eff} (BM) = 1.94; Δm (mhocm^2 mol^{-1}) = 19.

Copper Complex of Cu-h: Mol. Formula: $C_{31}H_{36}CuN_2O_7$. MW = 596. Yield: 75%. Anal. Calcd for $C_{31}H_{36}CuN_2O_6$: C, 62.45; H, 6.09; Cu, 10.66; N, 4.70. Found: C, 62.29; H, 5.91; Cu, 10.51; N, 4.59. FAB mass spectrometry (FAB-MS): m/z 597 [M+1]. μ_{eff} (BM) = 1.92; Δm (mhocm^2 mol^{-1}) = 18.

Biological Studies

Antimicrobial activity

The investigated compounds antibacterial properties *in vitro* against bacterial and fungal species were evaluated. The bacterial and fungal cultures were inoculated in broth (inoculation medium) the day before the experiment and incubated at 37 °C overnight. To achieve equal distribution, an inoculation medium containing a 24 hrs growing culture was added aseptically to the nutritional medium and carefully mixed. This solution was put into petri dishes (25 mL each dish) and allowed to cool to room temperature. Using suitable sterile tubes, wells (6 mm in diameter) were cut in the agar plates. The wells were then filled with 0.1 mL of the test chemicals dissolved in DMSO (200 mM/mL) to the agar surface. To aid in the spread of the medication solution, the plates were let to stand for an hour. The plates were then incubated for 24 hrs for bacteria and 48 hrs for fungi at 37 °C, and the diameter of the inhibitory zones was measured. The serial dilution approach was used to obtain the minimum

inhibitory concentrations (MICs). The MIC was determined as the lowest concentration (mg/mL) of chemical that inhibited bacteria growth after 24 hrs of incubation at 37 °C and fungal growth after 48 hrs of incubation at 37 °C. The amount of DMSO in the medium had no effect on the growth of any of the bacteria that were tested.

Antioxidant Assay

Individual samples were evaluated at a final concentration of 10 µM. The solution contained 1 mL of DPPH (60 µM diphenylpicrylhydrazyl radical) and various concentrations of antioxidant solutions of ligands and their complexes, resulting in a final DPPH concentration of 30 µM. The mixtures were thoroughly mixed and left to stand for 30 minutes at 25°C in the dark. The absorbance of the resultant solutions was measured at 517 nm against a blank sample containing only DPPH, which served as the negative control; the positive control included rutin and vitamin C.

$$\text{Scavenging effect (\%)} = \frac{(A_0 - A_1)}{A_0} \times 100$$

Where, A_0 is the absorbance of the control reaction and A_1 is the absorbance in the presence of the samples or standards.

Inhibition of Superoxide Radicals by Riboflavin Photoreduction Method

The NBT reduction method was used to assess superoxide scavenging. Phosphate buffer (6.7 mM, pH 7.8) was added to 3 mL in a test tube to modify the reaction mixture including EDTA (0.1M), 0.0015 % NaCN, riboflavin (0.12 mM), NBT (1.5 mM), and various concentrations of test sample and total volume. After 15 min of uniform illumination under an incandescent light, the optical density of the tubes was measured at 530 nm. By comparing the absorbance of the control and experimental tubes, the percentage inhibition of superoxide production was calculated. Using the formula, the % inhibition was obtained.

$$\text{Percentage inhibition} = \frac{((C - T) \times 100)}{C}$$

Where, C and T are the optical density of the control and test samples respectively.

DNA Binding Activity

UV–Vis Absorption Spectroscopy: Absorption spectra were recorded on Systronics 2201 Double beam UV–Vis, spectrophotometer using 1 cm quartz micro-cuvettes. The concentration of the complexes was fixed constant (10 µM) while the concentration of CT-DNA was varied from 0 to 10 µM in absorption titrations. A DNA blank was inserted in the reference cell to wipe out any absorbance from DNA at the wavelength being measured. The binding constants (K_b) for complex [Cu-L] were calculated from spectroscopic titration data using Eq:

$$[DNA] / (\varepsilon_a - \varepsilon_f) = [DNA] / (\varepsilon_b - \varepsilon_f) + 1/ (\varepsilon_a - \varepsilon_f)$$

The 'apparent' extinction coefficient (ε_a) was obtained by calculating $A_{obsd}/[Cu]$. The terms (ε_f) and (ε_b) correspond to the extinction coefficients of free (unbound) and the fully bound complexes, respectively. A plot of [DNA] / ($\varepsilon_a - \varepsilon_f$) versus [DNA] will give a slope of $1/(\varepsilon_a - \varepsilon_f)$ and an intercept of $1/K_b(\varepsilon_a - \varepsilon_f)$. Kb is the ratio of the slope to the intercept.

Viscosity measurements: Viscosity tests were performed using an Ostwald viscometer that was submerged in a thermo stated water bath that was kept at 30 ± 0.1 °C. At room temperature, the viscosity measurements were taken. To minimize the complications caused by DNA flexibility, DNA samples of roughly 0.5 mM were produced by sonication. For each sample, flow time was measured three times with a digital stopwatch, and an average flow time was determined. Each experiment was repeated three times to determine the average flow time. The data was shown as (η/η_0) versus binding ratio, with hrs

representing the viscosity of DNA in the presence of complex and h representing the viscosity of DNA alone. Viscosity values were calculated after correcting the flow time of buffer alone (t_0), $\eta = (t - t_0)/t_0$.

Thermal denaturation (T_m) Studies: A Shimadzu 160 spectrophotometer with a thermostatic cell holder was used to study thermal denaturation. By retaining the concentrations of DNA and [Cu-L] (30 µM) in a 1:1 ratio, the Tm value of CT-DNA was calculated in the absence and presence of metal complexes. While the absorbance changes at 260 nm were observed, the DNA samples were continually heated at a rate of 1 °C/min temperature increase. The midpoint of the melting curves was used to calculate the melting temperature (Tm), which is defined as the temperature at which half of the total base pairs are unbound. Tm values were obtained by subtracting Tm of free DNA from Tm of complex DNA.

Assay of DNA cleavage

For DNA cleavage study, buffer solutions of 50 mmol Tris-HCl/18 mmol NaCl in distilled water (pH 7.1) and Tris-acetic acid-EDTA in distilled water (pH 8.3) were used. Using agarose gel electrophoresis in the presence of H_2O_2, the extent of cleavage of supercoiled pUC18 DNA (33.3 mM, 0.2 mg) to its nicked circular form was evaluated. The gel electrophoresis tests were carried out at 35 °C for 1.5 hrs with the following ingredients: 10 mM pUC18 DNA, 5 mM each complex, 1 mM H_2O_2 in 50 mM tris-HCl buffer (pH = 7.2), and 30 mL double distilled water. The samples were electrophoresed for 2 hrs at 50 V on 1% agarose gel using tris-acetic acid-EDTA buffer (pH = 8.3). After electrophoresis, the gel was stained using 1 mg/cm^3 ethidium bromide and photographed under UV light.

Anti-inflammatory Activity

The anti-inflammatory activity of metal complexes was determined by using carrageenan induced paw edema method. The rats were divided into four groups of six rats each. Group I received normal saline and served as control. Group II and III received the doses of 100 and 200 mg/kg bw of the metal complexes, respectively. Group IV received the standard drug, Indomethacin 10 mg/kg bw. Edema was induced by injecting 0.1 ml of carrageenan (1% w/v; Sigma, USA) in normal saline into the subplantar region of the left hind paw after 1 h of drug administration. The paw volume was measured with the help of mercury replacement plethysmometer (Model 7140, UGO Basile, Italy) first at 0 h and then at 1, 2, 3, and 4 h after administration of drugs. The percentage inhibition of edema compared with that of the control was taken as anti-inflammatory activity. The percentage inhibition of edema was calculated by the formula;

$$\text{Percentage inhibition of edema} = \frac{(A - B)}{A} \times 100$$

Where, A represents the paw volume of the control at 3 hrs and B represents the paw volume of the test drug treated at 3 hrs.

Anti-proliferative assay

The target compounds, which were chrysin derivatives of copper complexes, were put through anti-proliferative activity tests *in vitro*. The growth inhibitory effects on the cell lines were determined using the MTT [3-(4,5-dimethylthiazol-2-yl)-2,5-diphenyltetrazolium bromide] test (Hela and MCF-7).

α-Glucosidase inhibitory assay

Pistia Brueggeman and Hollingsworth used a slightly modified approach to test the α-glucosidase inhibitory efficacy of the metal complexes. The copper complexes were prepared at different concentrations (20–400 µg mL^{-1}); 100 mL of phosphate buffer along with enzyme (α-glucosidase) concentration of 10 µL were incubated for 20 min at RT. After incubation time, the inhibitory action was started with slow addition of pNPG (β-Galactosidase) (substrate) of 10 µL and again incubated for 30 min. The inhibitory action was terminated with drop by drop addition of 50 µL (0.01 N) Na_2CO_3 and absorbance was noticed at 405 nm using a multi-well plate reader. Enzymatic activity was calculated as:

$$IC_{50} = \frac{(OD_{Blank} - OD_{Sample})}{OD_{Blank}} - 100$$

The IC_{50} values were calculated and tabulated for the prepared complexes against α-glucosidase inhibitory efficiency.

Cholinesterase activity assay

The chrysin derivative inhibitory activity against acetylcholinesterase (AChE) and butyrylcholinesterase (BuChE) were determined using a modified Ellman's method [23]. The inhibitory concentration (IC_{50}) was determined by plotting of absorbance against inhibition (%) curve. IC_{50} values were calculated for a given sample, the concentration at which the sample inhibits half of the maximum biological response. The substrates, acetylthiocholine iodide and butyrylthiocholine iodide, were utilized for the measurements. 5,5′-Dithio-bis(2-nitrobenzoic) acid (DTNB) was used to measure anticholinesterase activity. Stock solutions of the 1,10-phenanthroline derivative, galanthamine and rivastigmine, in DMSO were prepared at 200 μg mL^{-1}. The reaction mixture consists of 100 μL of 0.1 μM phosphate buffer (pH 8.0), 10 μL of sample solution (chrysin derivative) and 20 mL AChE (2.45×10^{-4} U μL^{-1}) (or 3.10×10^{-4} U μL^{-1} BuChE) solution and were mixed and incubated for 15 min at 25 °C. About 10 μL of DTNB solution was prepared by adding 2.0 mL of pH 7.0 and 4.0 mL of pH 8.0 phosphate buffers to a mixture of 1.0 mL of 16 mg mL^{-1} DTNB and 7.5mg mL^{-1} $NaHCO_3$ in pH 7.0 phosphate buffers. The reaction was initiated by addition of 10 μL (7.0 mM) acetylthiocholine iodide or 0.79 mM butyrylthiocholine iodide. The activity was measured by following the yellow color produced as a result of the thioanion produced by reacting the enzymatic hydrolysis of the substrate with DTNB. DMSO was used as solvent. The standards galantamine and rivastigmine were chosen as standards.

Catalase activity

CAT catalyses the spread of hydrogen peroxide (H_2O_2) and competes with GPx for the same substrate. It has long been thought that CAT is the primary scavenger of intracellular H_2O_2 generated by oxidative stress. The amount of enzyme that liberates half the peroxide oxygen from H_2O_2 in seconds at 25 °C was measured spectrophotometrically at 250 nm and expressed as unit/mg of protein [24].

Results And Discussion

Chemistry

The production of chrysin derivatives of copper complexes for therapeutic purposes was the focus of this study. The removal of oxygen atom by nitrogen atom in the ring C by the utilization of different n-propyl amine / n-pentyl amine to arrive different structural motifs could lead to 5,7-dihyroxyflavone derivatives with desirable structural features were also increased lipophilic character and stability in medium. Thin-layer chromatography was used to track the reactions development (TLC). Elemental analysis, UV, FT-IR, FAB-MS, ^{1}H & ^{13}C NMR and ESR spectral data observations were used to elucidate the chemical structural properties of synthesized chysin derivatives of ligands and copper complexes. Chemical transformations were used to create pharmacologically active moieties (-C-C and -C-N-C-) [25] and structure elucidation was determined utilizing the preceding procedures. All of the chrysin derivatives produced agreeable analytical and spectroscopic results that matched their indicated structures perfectly.

Molar conductance

The copper complexes molar conductance values were measured in DMSO solution for the 0.001M solutions. The values fall in the range of 10–26 Ω^{-1} cm^2 mol^{-1}, which is the expected range for non-electrolytes [26]. As a result, the current complexes are non-electrolytic in nature, as indicated by the acetate group role in coordination. The chemical analysis confirmed that the CH_3COO^- ion is not precipitated when $FeCl_3$ is added. There were no electrolytic characteristics in any of the complexes.

Ultraviolet spectra

The electronic spectra of chrysin ligand (Fig. S1) have an intensive band at 322 nm is related to the absorbance of the B ring (cinnamoyl system), whereas the band at 238 nm is related to the л → л* transition absorbance (cyclic aromatic benzoyl system) in the A ring. The electronic spectrum of the corresponding chrysin copper complex in DMSO reveals a broad band at 518 nm assignable to $^2B_{1g} \rightarrow {}^2A_{1g}$ transition (Fig. S2) which is characteristic of distorted square planar environment around the copper(II) ion.

Infrared spectra

In the IR spectrum of chrysin, valance carbonyl group vibrations coupled with the double band in the γ-benzopyrone ring at 1633 cm^{-1} and absorption bands situated at 1612, 1544 and 1425 cm^{-1} related to carbon vibration in benzene and γ-pyrone rings (valance vibrations C = C) occur (Fig. S3). The IR spectrum of the ligand shows a higher peak υ(C=N) in the 1643-1630 cm^{-1} range. Both complexes have υ(C=N) bands at 1631-1591 cm^{-1} [27] and the υ(C=N) bands in the complexes are shifted to lower energy regions relative to the free ligands, indicating that azomethine nitrogen is one of the coordinating atoms in the Schiff bases. Infrared spectra of copper complexes reveal some new bands in the 481-451 and 450-411 cm^{-1} regions, which may be due to the formation of M-O and M-N bands, respectively [28]. The acetate group may be responsible for the band at 521 cm^{-1} in the [Cu-L(OAc)(H_2O)] complex spectrum υ(M-O).

NMR spectra

The ^1H NMR spectrum of the ligand 3g shows (Fig. S4) different signals and are assigned as follows: 6.57 (1H, s, -CH), 7.1 (1H, s, -CH), 7.12-7.36 (5H, m, Ar-H, -CH), 3.06 (2H, t, $-CH_2$), 1.55 (2H, m, $-CH_2$), 1.29 (2H, m, $-CH_2$), 1.31 (2H, m, $-CH_2$), 0.94 (3H, t, $-CH_3$), 5.11 (2H, s, $-CH_2$), 6.00-6.53 (4H, m, -CH), 10.98 (1H, s, D_2O exchange, -OH) 10.51 (1H, s, D_2O exchange, -OH) respectively.

The ^{13}C NMR ligand 3g (Fig. S5) shows different signals and are assigned as follows: 162.1 (C_2), 97.3 (C_3), 182.1 (C_4), 161.4 (C_5), 92.1 (C_6), 164.5 (C_7), 101.5 (C_8), 146.6 (C_9), 111.6 (C_{10}), 134.1 (C_{11}), 126.6 ($C_{12, 16}$), 128.9 ($C_{13, 15}$), 128.0 (C_{14}), 44.5 (C_{17}), 28.1 (C_{18}), 29.5 (C_{19}), 22.6 (C_{20}), 14.4 (C_{21}),38.8 (C_{22}), 122.6 (C_{24} - C_{26}), 108.6 (C_{25} - C_{27}) respectively. All the protons were found as to be in their expected region. Based on literature results, all other ligands had similar spectral assignments.

ESR spectra

The copper complex ESR spectra was measured in DMSO at 300 and 77 K (Fig. S6 and Table S1). Due to the tumbling motion of the molecules, the spectra at 300 K reveals one prominent absorption band at high field that is isotropic. In the frozen state, however, this complex presents four well-resolved peaks in the low field region with low intensities and one powerful peak in the high field region. The copper complex has a magnetic moment of 1.96 BM, equating to one unpaired electron, showing that it is mononuclear in nature, according to the magnetic susceptibility value. Due to the ms = ±2 transitions, there was no half field signal in the spectrum at 1600 G, ruling out any Cu–Cu interaction [29]. Table S1 displays the ESR spectrum data. In the current Cu-complex, the value of g < 2.3 indicates that the copper-ligand connection is covalent and that the unpaired electron has delocalized into the ligand. The axial symmetry with the unpaired electron in the $d_{x^2-y^2}$ orbital [30] is described by the trend of g (2.25) > $g_\perp$ (2.04) > g_e (2.0036). The observed g values for the current Cu(II) complex are g (2.26) > $g_\perp$ (2.05) > g_e (2.0036), indicating that the unpaired electron is in the $d_{x^2-y^2}$ orbital. The order of the A and $A_\perp$ values: A (147) > $A_\perp$ (52) also indicates that the complex has distortion square planar geometry and that the system is axially symmetric. Researchers discovered a strong link between the f factor (g /A) and the SOD-like activity of copper complexes. CuZnSOD has f value of 160 cm, suggesting a tetrahedral distortion from square planar geometry, which is one of the properties that improve the enzyme's catalytic activity. Copper complexes have f values of 154, 156, 152 and 145 cm, respectively, based on the above ESR spectral data. As a result, our synthesized copper complexes have a significant square planar distortion, indicating that they are likely to have strong SOD activity. The current EPR studies demonstrate that g is less than 2.3 in all cases, indicating that the copper

complexes are covalent in nature; they also show that g is in the range of 2.21-2.26, indicating that these complexes contain mixed copper–nitrogen and copper-oxygen links.

Mass spectra

Mass spectra can be used to determine a compounds structure. The mass spectra of the ligand (3h) and its copper complex [Cu-h(OAc)(H_2O] were compared, as were their stoichiometric compositions. The strength of these peaks is proportional to the ions' stability and abundance. The ligand (3h) exhibits a molecular ion peak at 457 m/z (Fig. S7), whereas its copper complex (Cu-h) has a molecular ion peak at 597 m/z (Fig. S8), suggesting that the metal complexes are stoichiometrically [Cu-h(OAc)(H_2O]. FAB-mass investigations of the various complexes confirm that the values determined from the molecular formula assigned to these complexes agree closely with the values calculated from the elemental analysis. Similar mass spectrum characteristics were assigned to other ligands and their copper complexes. The stoichiometry is confirmed by the mass spectra of complexes.

Themogravimertic analysis

The thermal stability of copper complexes can be determined using TGA. The thermogravimetric profile revealed the distinct structural moieties present in the copper chelate, such as lattice acetate or coordinated acetate molecules, anions, molecular fragments and metal oxide as a residue. Under nitrogen atmosphere, the thermogravimetric profile of copper complexes was measured up to 800 °C at a heating rate of 10 °C/min. There was no breakdown below 225 °C in the copper complex, indicating that there were no water molecules present. Then, in the temperature range of 250–410 °C, the breakdown position was found, which corresponds to the partial decomposition of the ligand system. Furthermore, the divergence observed between 350 and 470 °C indicates that the full decomposition of the ligand results in copper oxide (CuO) as a residue, coupled with a little amount of ash. For all copper chelates, identical thermogravimetric properties were reported. In catalytic applications, thermal stability is an important structural characteristic. As a result, the observed manner of disintegration in relation to temperature and excellent agreement with the suggested structural formulas of the copper chelates as represented in Scheme 1 are concluded.

X-ray powder diffraction spectra

The X-ray diffractogram of the ligand and its copper complexes were reported in the region of 5° to 80° 2 theta values. The ligand and its copper chelates PXRD patterns revealed well-defined crystalline patterns with varying crystallinity. Due to the creation of copper complexes, there were additional peaks in the chelates when compared to the ligand. In the supplemental information, the copper chelate XRD spectrum was provided (Fig. S9). Several attempts at growing single crystals suitable for X-ray crystallography, such as crystallization utilizing solvent combinations and low temperatures, failed.

SEM analysis

The surface morphology (SEM) of the copper complexes displayed several morphologies. The particle sizes of the Cu(II) complexes were within the range of a few microns in diameter (Fig. S10). Particles smaller than 100 nm in size were also found to shape larger agglomerates in groups. These facts are in good agreement with the results of the XRD collected for powder.

Antimicrobial activity

The antimicrobial properties of the synthesized compounds were tested against bacterial species and fugal species, using the well diffusion technique against a variety of microorganisms [31-33]. Then, using a serial dilution approach, the minimum inhibitory concentrations (MIC) were calculated. The antibacterial and fungal activity of the ligands and copper complexes were compared to standard antibiotic, Vancomycin, Ampicillin, Nystatin and Bavstatin. The antibacterial action of the compounds may be attributable to heteroaromatic residues in this investigation. The antibacterial activity of complexes is higher than that of free ligands, according to a comparison study of ligands and their complexes. Compounds with > C = N group have better antibacterial action than those with > C = C < group. Certain microbes can develop even in the absence of

oxygen. As a result, molecules with > C = C < group that are capable of absorbing O_2 are unrelated to the growth of microbes. Table 1 show the observed results and summarizes them. In the present investigations, the synthetic heterocyclic compounds contain hydroxy group at different positions of A and B rings has also been exhibited higher antibacterial activity. The biological activity of chemicals, particularly Cu-g, may be attributed to the distribution of cell wall constituents, inhibition of protein synthesis, inhibition and prevention of nucleic acid replication, interference with metabolic pathways, and microorganism death caused by cell wall breakdown. The following are the primary physico-chemical and structural properties that are responsible for antimicrobial activity: (i) The Liphophilic property, which permits molecules to travel across lipid membranes; (ii) The presence of a –C-O-C- group in the molecule forms an energetic hydrogen bond with cell wall elements, increasing activity; (iii) The spatial orientation of the chemical that allows chrysin derivatives to interact with biomolecules in the system in a favourable manner; (iv) The presence of uncoordinated donor atoms aids in the identification of cell wall locations and enhances solubility.

Table 1 Antimicrobial activity of ligands and their copper complex (MIC values µg/mL)

Compounds	*E. Coli*	*k. pneumonia*	*S. Typhi*	*S. Aureus*	*P. aeruginosa*	*A. Niger*	*R. Stolonifer*	*A. flavus*	*C. Albican*	*R. bataicola*
Vancomycin	6	14	12	8	10	-	-	-	-	-
Ampicillin	12	10	8	6	4	-	-	-	-	-
Nystatin	-	-	-	-	-	10	16	8	12	14
Bavstatin	-	-	-	-	-	14	10	8	12	6
3a	69	86	75	83	67	79	81	89	86	74
3b	63	76	85	75	63	89	68	61	91	77
3c	65	65	68	73	58	61	74	65	57	65
3d	62	69	69	72	59	67	61	82	55	69
3e	69	84	72	81	66	78	86	87	84	71
3f	64	73	84	76	62	87	66	59	88	81
3g	58	65	67	71	56	59	71	63	55	66
3h	59	67	66	69	58	65	58	81	56	67
Cu-a	40	44	39	37	39	53	46	39	51	39
Cu-b	33	26	37	39	31	35	29	30	39	37
Cu-c	28	24	35	26	26	43	35	29	33	34
Cu-d	29	41	36	37	27	45	33	31	39	35
Cu-e	39	41	36	34	37	51	41	36	49	37
Cu-f	30	23	36	34	28	32	26	28	36	36
Cu-g	25	21	31	23	23	34	33	27	32	31
Cu-h	26	37	33	32	24	36	29	22	34	34

Antioxidant

Antioxidants that can scavenge DPPH radicals have gotten a lot of interest. Antioxidant compounds may provide protection against rheumatoid arthritis and inflammation, as well as contribute to the development of potentially beneficial medications.

The greater the hydrogen-donating ability, the lower the IC_{50} value. Cu-g copper complexes have strong antioxidant activity due to the presence of an OH group and efficient hydrogen donors that stabilize unpaired electrons and scavenge free radicals. The addition of an OH group to the ligand system significantly improves the antioxidant efficacy of the complexes, and the antioxidant behaviour of the complexes can be increased by carefully selecting the substituents on the ligand.

In this investigation, the copper complex of Cu-c had a substantially higher DPPH scavenging activity (68%) than other ligands and their complexes at a concentration of 10 µM. Vitamin C and Rutin, which were used as positive controls, demonstrated 58% and 67% DPPH scavenging, respectively. The strong antioxidant activity of copper complex of Cu-g compared to free ligands and other copper complexes could be attributed to copper coordination in the 4^{th} and 5^{th} positions of the condensed ring system (A and C ring), which increases its ability to stabilize unpaired electrons and hence scavenge free radicals. Furthermore, the inclusion of the pyrrole moiety to the chrysin derivatives increased the antioxidant activity even more. The coordination of copper in the 3^{rd} and 4^{th} positions has demonstrated higher activity than Cu-h, which could explain why the Cu-g complex showed higher antioxidant activity than vitamin C. Cu-d copper complexes may be considered as new intriguing lead candidates for further design and synthesis of antioxidants, according to the researchers.

The comparative inhibitory values of ligands and their complexes against standards are summarized Table 2 and shown in Fig. 1.

Table 2 Antioxidant properties of ligands and copper complexes.

Compounds	IC_{50}(µM)
3a	0.52
3b	0.51
3c	0.47
3d	0.46
3e	0.50
3f	0.48
3g	0.42
3h	0.43
Cu-a	0.37
Cu-b	0.35
Cu-c	0.33
Cu-d	0.37
Cu-e	0.34
Cu-f	0.33
Cu-g	0.30
Cu-h	0.31
Rutin	0.28
Vitamin C	0.34

SOD Activity

The development of SOD mimics for the scavenging of superoxide ($O_2^{\bullet -}$), a precursor to reactive oxygen and nitrogen species (RONS) that contribute to oxidative stress, has piqued interest. The copper(II) complexes SOD mimetic activities were presented in Fig. 2 and summarized in Table 3. The electron scavenging activity of complexes containing an electron withdrawing group on the ligand is higher.

Cu-g has a stronger SOD activity than the other complexes because it has an electron withdrawing group (pyrrole). Because of the stronger axial connection, a higher contact between superoxide ion and Cu(II) complex is induced, resulting in improved catalytic activity. Furthermore, amine substituted ligands with an electron withdrawing group stabilize the Cu(I) oxidation state created during superoxide dismutation, which then interacts with the superoxide ion to produce hydrogen peroxide. Because the geometry of copper in the SOD enzyme moves from distorted square planar geometry to distorted square planar geometry, the distorted geometry of these complexes may favour the geometrical change that is required for catalysis. Complexes SOD activity is determined by their coordination environment, ligand exchange availability and catalytic efficacy. SOD activity and antioxidant defence mechanisms have been altered by the addition of substances such as n-propyl amine or n-pentyl, among others.

Copper(II) is thought to be quickly reduced to copper(I) when cysteine or glutathione is present. Cysteine's sulphydryl group (RSH) is easily oxidized to become cystine (RSSR). Several redox proteins go through this form of intercellular conversion. The reduced copper(I) is converted to copper(II) in the second stage, with $O_2^{\bullet -}$ being converted to hydrogen peroxide at the same time. SOD mechanism that represent the reaction sequence are as follows:

SOD Mechanism:

First Step

$$Cu^{2+} + RSH \longrightarrow Cu^{+} + RSSR$$

Second Step

$$Cu^{+} + O^{-2} + 2H^{+} \longrightarrow Cu^{2+} + H_2O_2$$

Table 3 Superoxide dismutase activity of compounds (IC_{50} values).

Compounds	IC_{50}(μM)
Cu-a	0.34
Cu-b	0.30
Cu-c	0.26
Cu-d	0.28
Cu-e	0.24
Cu-f	0.20
Cu-g	0.16
Cu-h	0.18
Native SOD	0.04

DNA binding studies

One of the possible mechanisms for copper complexes cytotoxic activity is their interaction with DNA (along with a variety of other targets found in living cells). It will be useful to investigate the DNA molecule binding of Cu(II) complexes once they contain the biologically important chrysin moiety. UV-Vis, spectral fluorescence, viscosity experiment, electrochemical studies and DNA melting techniques were used to investigate the binding of its copper complexes with CT-DNA.

Absorption titration experiment: UV-Vis absorption spectroscopy is one of the most widely used and effective tools for analysing metal complexes interactions with DNA. DNA is a therapeutic target molecule with a unique interaction between its planar aromatic core and base pairs, which is coupled to a metal complex via intercalation. The electronic absorption spectra of the copper complex were measured in the absence and presence of DNA. At room temperature, CT-DNA interactions with its copper complexes were studied using UV-Vis absorption spectroscopy in a Tris-pH 7.2 buffer. The electronic spectra of copper complexes are displayed as illustrative examples in Fig. 3, with CT-DNA introduced gradually. In the absence and presence of increasing amounts of CT-DNA, the electronic spectra of copper complexes are saved. The copper complexes absorption band at 436 nm showed hypochromism and bathochromism after incremental amounts of CT-DNA were added, as seen in Fig. 3. This result suggests that copper complexes interact with CT-DNA predominantly by non-covalent intercalation [34].

Competitive binding with EB: Spectral titration fluorescence measurements at room temperature in the Tris-HCl buffer at pH 7.2 were also used to investigate the interactions between the ligands and their copper complexes. Fluorescence displacement experiments with ethidium bromide (EB) have been widely used in these fluorescence titration investigations to explain the interaction between CT-DNA and copper complexes. Due to the development of the CT-DNA / EB copper complex in the presence of CT-DNA, EB emits bright fluorescence through strong binding intercalation mode. In the absence and presence of Cu(II) complexes, the fluorescence emission spectra of the CT-DNA / EB group are presented in Fig. 4. When quenchers (copper complexes) were added to the CT-DNA / EB system, the fluorescence intensity of the system fell dramatically, as shown in Figure, showing that quenchers can displace EB from the CT-DNA by competitive binding, which is a frequent property of DNA intercalators [35]. This result indicated that the quenchers in discussion would bind to CT-DNA in an intercalative mode. The binding constants for the CT-DNA / quencher systems were determined using the fluorescence spectral titration data. For these systems, a linear plot of [DNA] / (εb-εf) versus [DNA] is shown in Fig. 4A and B. The binding constants that have been defined thus far are summarized in Table 4. The copper complexes under research have much lower binding constants than the standard intercalator EB (2.98×10^5 M^{-1}). These quenchers used linear Stern-Volmer plots to quench the fluorescence of EB / CT-DNA (Fig. 4A and B), and the quenching constants, as well as the apparent binding constant values, are listed in Table 4. Such findings showed that in the present case, the binding constant values of the copper ion complexes make the binding relatively stronger with CT-DNA. These results revealed that in this case, the copper ion complexes binding constant values make CT-DNA binding relatively stronger.

Table 4 CT-DNA binding constant (K_b), quenching constant (K_q) and apparent binding constant (K_{app}) values of copper complexes.

S. No	Copper complexes	K_b (M^{-1})	K_q (M^{-1})	K_{app} (M^{-1})
1	Cu-e	2.20×10^4	4.12×10^3	2.98×10^5
2	Cu-f	2.87×10^4	5.89×10^3	3.46×10^5
3	Cu-g	4.55×10^4	8.31×10^3	3.81×10^5
4	Cu-h	3.29×10^4	6.57×10^3	3.35×10^5

Viscosity measurements: Optical measurements alone are insufficient to deduce how small molecules bind to DNA. The viscosity experiment is a useful method for evaluating metal complexes binding to DNA. To determine the interactions between the copper complex and the DNA, viscosity measurements were taken using intercalation, electrostatic and groove binding

modes. In the absence of crystallographic structural data, hydrodynamic measurements based on changes in length (viscosity and sedimentation) are regarded the most significant binding information. Complexes have a binding affinity for DNA, according to the proportionate changes in viscosity. The DNA helix must be elongated and the DNA viscosity must be raised in a conventional intercalation mode. The viscosity varies in lower amounts when electrostatic or groove surface binding is used. By intercalating the double helix of DNA, ethidium bromide, a well-known DNA intercalator, greatly increases relative viscosity. There is a significant increase in viscosity when DNA is added to the copper complexes (Fig. 5). The increased viscosity showed that the complexes engage by intercalation binding, which is supported by electronic spectrum features. The copper complex (Cu-g) has a higher affinity for binding DNA than the other copper complexes, according to the results of the experiments. The strong л-л stacking interaction between these complexes and DNA is caused by the planar chrysin derivatives ligand intercalating into the base pairs of DNA.

Electrochemical studies: Cyclic voltammetric studies on the Cu^{+2} [Cu-L(OAc)(H_2O)] complex with chrysin derivatives revealed a quasi-reversible one-electron redox mechanism involving the Cu^{+2} / Cu^{+} couple at E_{pa} = 0.05 and E_{pc} = 0.20 V, within the potential scan range of +1.0 to −1.0 V. A significant decrease in both anodic and cathodic peak current, a positive shift in $E_{1/2}$, and a difference in peak potential (E_p) with the addition of CT-DNA to the copper complex (Fig. 6) suggested slow diffusion at the electrode surface due to copper complex binding to the electrode surface via intercalation of phenyl rings and electrostatic interactions between the negatively charged phosphate backbone and positively charged copper ion. The copper complex had a high level of cytotoxicity against the HeLa and MCF-7 cell line.

DNA melting studies: Copper complexes affinity for the double DNA helix has been shown to raise the melting temperature of CT-DNA, at which the double helix denatures into single-stranded CT-DNA. Melting temperature was used to determine the interaction of complexes with CT-DNA through intercalation. From 30 to 90 ℃, the melting temperature of metal complexes with CT-DNA was controlled using an absorbance at 260 nm. Fig. 7 and Table 5 show the CT-DNA melting curves in the presence and absence of the copper complex. Tm values for free CT-DNA are 65 ℃ and 75 ℃ when [Cu-L] is present. When the complex was added to CT-DNA, a minor shift in the DNA melting temperature or denaturation temperature (ΔT_m) was observed. Since the extinction coefficient of double-helical DNA at 260 nm is much lower than that of single-stranded DNA, melting the helix causes an increase in absorption at this wavelength. Monitoring the absorbance of DNA bases at 260 nm as a function of temperature can thus be used to evaluate the helix to coil transition temperature (T_m). The л-stacking interaction between complex and base pairs of DNA caused the de-stabilization of DNA structure. The organic structural centre (Chrysin derivative) and copper coordination can have a big impact on nucleic acid structure, conformation, stability and affinity. The intercalation of complexes into the double helix has been shown to increase the helix melting temperature, which is the temperature at which the double helix denatures into single-stranded DNA [36]. All copper complexes followed a similar pattern.

Table 5 Melting temperature in the absence (DNA alone) and in the presence of different copper complexes.

S. No	Copper complexes	T_m (°C)
1	Absence of copper complex	70
2	Cu-a	83
3	Cu-b	85
4	Cu-c	89
5	Cu-d	87
6	Cu-e	84
7	Cu-f	87
8	Cu-g	92
9	Cu-h	90

DNA cleavage studies

The efficiency of the cleavage of the pUC19 DNA with Schiff base Cu(II) complexes was investigated using a method known as "gel electrophoresis" with H_2O_2 present as an external cofactor agent, and the results obtained are shown in Fig. 8. The selective transformation of the cleavage of the extremely coiled plasmid structure (Form I) under physiological conditions resulted in the formation of a form of open circular DNA (Form II), as shown in Fig. 8. Furthermore, in the presence of H_2O_2, the investigated copper(II) complexes DNA cleavage activities are thought to be the result of the formation of hydroxyl free radicals, which are involved in deoxyribose moiety oxidation and hydrolytic cleavage in the phosphate-sugar backbone [37]. The DNA cleavage efficiency of the copper(II) complexes compared to that of the control is dependent on their efficient DNA-binding ability. As can be seen from the figure, in the case of Cu(II) complexes there is a significant increase in band strength for open circular form compared with that of the other copper complexes.

Anti-proliferative activity

Using the conventional MTT assay technique, the anti-proliferative effects of chrysin derivatives of copper complexes Cu-a to Cu-h were investigated *in vitro* on human cancer cell lines HeLa and MCF-7. The synthesized compounds IC_{50} values were measured against cancer cell lines. When compared to chrysin and standard, the copper complexes showed inhibitory efficiency against cell lines during anti-proliferative screening. The Cu-e, Cu-f and Cu-h compounds have a significant cytotoxic efficacy due to their structural core (heterocylic moiety and aromatic fused ring and conjugation) responsible for activities and their IC_{50} values are slightly higher than standard and chrysin alone, respectively.

Natural materials with redox capabilities that can be utilized to activate a range of biological processes, control inflammatory action and cancer cell multiplication and prevent bacterial and fungal growth. The linear carbon chain, according to the literature, impeded drug binding in the active region of the protein, resulting in reduced anticancer activity. All other compounds and conventional medications had lower anticancer activity (Fig. 9) than the chrysin derivative with heterocyclic moiety (Cu-g) (bleyomycin). A tailor-made strategy was used to generate chrysin derivatives with active chemical pharmacopore such as hydroxyl, carbonyl and heterocyclic groups may be boosted solubility and extraordinary anticancer efficacy due to its DNA binding effectiveness, which causes disruptions in normal cell activity. Interactions with RNA/protein reduce cancer cell growth, which is followed by suppression of enzyme synthesis. The liphophilicity values imply selective permeability across cancer cell membranes, exposing anticancer potential through a variety of cellular activities (enzymatic, DNA synthesis, RNA synthesis, and so on) as well as cell death. Furthermore, the accessible donor atoms in chrysin derivatives were able to chemically activate DNA cleavage, increasing anticancer efficacy.

Anti-tubercular activity

The anti-tubercular effects of copper complexes (Cu-a to Cu-h) against Mycobacterium tuberculosis $H_{37}Rv$ were assessed *in vitro* using the broth dilution test technique [38]. Table 6 shows the anti-tubercular activity results. The results of antimycobacterial activity (Table 6) show that complexes are very active, with MIC values substantially below the MIC values of conventional medicines. Cu-g Copper Complex has been demonstrated to be a more effective antimycobacterial agent than ethambutol (due to the presence of pyrrole group at chrysin ring A position).

Table 6 *In vitro* anti-tubercular screening data of synthesized copper complexes MIC (μM).

S. No	Copper complexes	MIC (μM)
1	Cu-a	19
2	Cu-b	13
3	Cu-c	6
4	Cu-d	8
5	Cu-e	17
6	Cu-f	13
7	Cu-g	4
8	Cu-h	6
9	Isoniazid	2

Catalase activity (CAT)

In this research, the activity of CAT in hepatic cells was observed to be drastically lowered. Its conversion to molecular oxygen and water by CAT could be vital for cellular antioxidant defenses. Reduced antioxidant and detoxifying enzyme activity can lead to an increase in reactive oxygen species (ROS), which has been associated to a variety of disease pathologies [39]. In every case, copper complexes boosted CAT activity and reduced stress in liver cells.

Superoxide, hydrogen peroxide [H_2O_2] and lipid peroxides are removed by CAT, which helps to minimise oxidative stress. Reduced CAT activity has been associated with a variety of cancers [40]. A significant suppression of CAT behaviours was also observed in tumor-bearing mice, which could be ascribed to an increase in peroxides and a decrease in reduced glutathione levels. The treatment of cyclophosphamide further lowered these behaviours, indicating that cyclophosphamide had a deleterious impact on the host's antioxidant enzyme system. Copper complexes are displayed as CAT activity (Fig. 10). Copper complex (Cu-g) has a higher CAT activity than other copper complexes and standard compound (Ebselan), according to the findings of the preceding studies.

Reducing power

The capacity of the complexes to reduce can be employed to increase their antioxidant activity. Copper complexes were studied for their respective reducing capabilities. Chain initiation prevention, peroxide decomposition, hydrogen abstraction prevention and radical scavenging are only a few of the mechanisms that could explain the antioxidant activity. The [Cu-g(OAc)(H_2O)] complex exhibits a stronger overall antioxidant activity and lower reducing power than other Cu(II) complexes. Since then, it has been discovered that the lowering capacity of the aforementioned complexes is crucial in this study. As a result, these chemicals could be considered possible antioxidants that can generate copper(II) ligand radicals.

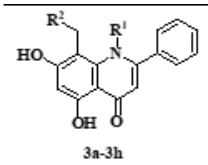
Partition Coefficient Determination

The capacity of organic/inorganic based compounds to cross lipid layers and restrict microbial growth was measured using partition coefficients (P). The shaking flask method was used to measure the partition coefficients of the generated compounds. Because of the extreme conjugated system and the varied substituted moiety contained in the compounds, the generated compounds have distinct P values. The synthesized chrysin derivatives of lidands had Log P values ranging from 3.91 to 6.71, showing lipophilic characteristics (Table 7).

The shaking flask method was used to determine the partition coefficients, or Log P, of bio-sensitive copper complexes. Copper complexes in the range of 2.53 to 5.84 have been found. When compared to other copper complexes, a copper complex with an electron withdrawing substituent and a pentyl and pyrrole moiety in the chrysin C ring showed a low Log P value (Table 7).

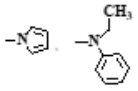
Because of their lipophilic nature, the complexes can penetrate the lipoidal bacterial membrane more efficiently than free ligands. Following clinical testing, these copper complexes could be employed as a chemotherapy drug.

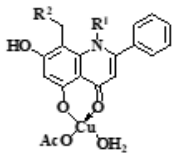
Table 7 Partition coefficients of ligands and its copper complexes.



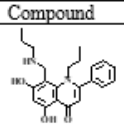
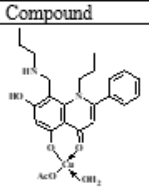
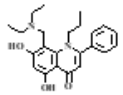
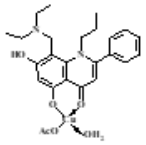
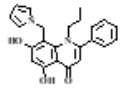
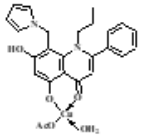
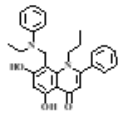
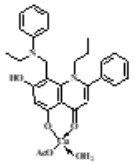
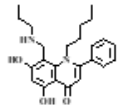
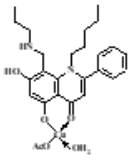
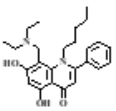
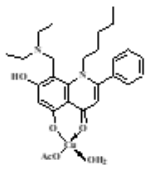
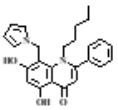
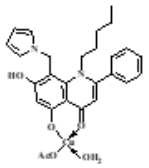
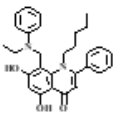
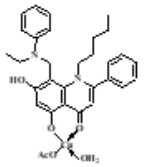
3a-3h

$R^1 = C_3H_7, C_5H_{11}$

$R^2 =$ $-NH(CH_2)_2CH_3$, $-N(C_2H_5)_2$, 



Cu-a to Cu-h

Ligands	Compound	Log P	Complex	Compound	Log P
3a		3.91	Cu-a		2.53
3b		4.14	Cu-b		3.44
3c		3.98	Cu-c		2.94
3d		5.87	Cu-d		4.62
3e		4.74	Cu-e		3.67
3f		4.97	Cu-f		3.86
3g		4.81	Cu-g		3.39
3h		6.71	Cu-h		5.84

Catalytic activity

For a quantitative gas chromatography study, the catalytic translation of benzene to phenol was performed in acetonitrile under argon atmosphere with hydrogen peroxide as the oxidant, copper complexes as catalysts, and o-dichlorobenzene as an internal norm using hydrogen peroxide as the oxidant, copper complexes as catalysts, and o-dichlorobenzene as an internal norm.

Solvent, catalyst (1 mM), substrate (1 M), a little quantity of oxidant, and o-dichlorobenzene (2 M) were added in that order. The reaction had a total volume of 2 ml and was agitated for 20 hours at 25 °C. Using too much triphenylphosphine and hexane halted the synthesis. The reaction mixture was filtered through a silica bed. The products were examined using gas chromatography. The proposed reaction mechanism is depicted in Scheme 2. In the instance of copper complex (Cu-g), the copper-hydroperoxo intermediate species is formed in the first step by reacting copper complex (Cu-g) with hydrogen peroxide. The copperehydroperoxo species undergoes haemolytic cleavage of the O-O bond in the second stage, resulting in a hydroxyl radical that interacts with benzene to form phenol (Scheme 2).

α -Glucosidase inhibition

Table 8 summarizes the results of the α-glucosidase inhibition research for the complexes, including the IC_{50} values. Chelation with copper acetates increased the inhibitory capability of α-glucosidase, demonstrating the critical role of the copper(II) centre during enzyme inhibition. This study indicates that the complexes will block α-glucosidase in a concentration-dependent manner. The copper(II) complex (Cu-g) was a powerful α-glucosidase inhibitor (IC_{50} = 0.19 μM), roughly 200 times more active than the conventional α-glucosidase inhibitor deoxynojirimycin (DNJ) (IC_{50} = 300 μM). The active site residues of α-glucosidases (imidazole and carboxy groups) interact with copper(II) ions through soft electron donors like imidazole nitrogen, which inhibits the enzyme. The presence and position of substituents in Cu(II) complexes influence the inhibition of α-glucosidase. The inhibitory values show that [Cu-L(OAc)(H_2O)] can more easily occupy active α-glucosidase sites than the usual, DNJ. [Cu-L(OAc)(H_2O)] can also create hydrogen bonds with the enzyme and regulate conformational changes, making α-glucosidase inhibition easier. As a result of its redox characteristics and molecular scaffolds, [Cu-L(OAc)(H_2O)] is an effective inhibitor of α-glucosidase.

Table 8 α-Glucosidase inhibition activity of copper(II) complexes and standard.

S. No	Complex/standard	IC_{50} (μM)
1	Cu-a	0.39 ± 0.02
2	Cu-b	0.36 ± 0.5
3	Cu-c	0.32 ± 0.2
4	Cu-d	0.35 ± 0.4
5	Cu-e	0.29 ± 0.03
6	Cu-f	0.27± 0.3
7	Cu-g	0.19 ± 0.04
9	Cu-h	0.26 ± 0.2
10	Copper-acetate	0.84 ± 0.01
11	DNJ	300 ± 0.5

Cholinesterase inhibitory activity

Cholinesterase inhibitors (ChEIs) are potential medications that increase cholinergic activity in the brain to improve memory, efficiency, and reduce the risk of psychiatric and behavioural disorders. Using galantamine and rivastigmine as reference compounds, the inhibitory activity on AChE and BuChE of the synthesized chrysin derivative (8-((1H-pyrrol-1-yl)methyl)-5,7-dihydroxy-1-pentyl-2-phenyl-quinolin-4(1*H*)-one (3g)) were measured using the modified Ellman technique. Donepezil, rivastigmine, and galantamine are examples of AChE inhibitors that are routinely used to treat cognitive impairments in people with Alzheimer's disease. Table 9 summarizes the inhibitory IC_{50} values for AChE and BuChE. The tightly conjugated (8-((1H-pyrrol-1-yl)methyl)-5,7-dihydroxy-1-pentyl-2-phenyl-quinolin-4(1*H*)-one showed the highest inhibition against AChE with an IC_{50}

value of 0.24 μM, similar to galantamine (IC_{50} = 2.41 μM). Rivastigmine (IC_{50} = 3.01 μM) also showed the best inhibition. The IC_{50} values obtained against BuChE showed that chrysin derivatives, as opposed to galantamine, serve as a selective inhibitor of AChE. Through hydrogen bonds, hydrophobic interactions, and a л–л interaction, phenolic chemicals interact with residues of amino acids that characterise the active site of AChE. Several hydroxyl groups in the phenolic molecule are expected to boost AChE inhibitory effect by increasing binding capacity. The fused aromatic nuclei with higher inhibitory AChE potencies are illuminated by the aromatic centre (conjugation) than their similar molecules with only one or two fused ring systems. The finest inhibitors have fused aromatic properties and operate as powerful AChE inhibitors. The azomethine moiety also enhances strong attachment to the AChE active site, which limits choline substrate hydrolysis. As a result, the azomethine, pyrrole and phenolic moiety, or lipophilic moieties on the conjugated aromatic core, may be the primary requirement for anti-AChE activity. From the perspective of multifunctional anti-AD medicines, this research finding may present potential for researchers to build novel effective inhibitors of ChEs by appropriately altering the pattern of substitution and also some pharmacophores. According to the selectivity index, the produced ligand may provide preferential inhibition of BuChE over AChE. However, more clinical trials are needed to determine the efficacy of the chrysin derivative in the treatment of Alzheimer's disease.

Table 9 *In vitro* inhibition IC_{50} values (μM) and selectivity index of compound and standards for AChE and BuChe.

Compound structure	IC_{50} (μM)		Selectivity Index=$IC_{50(BuChE)}/IC_{50(AChE)}$
	Ache	BuChe	
Ligand (3g)	0.24±0.10	3.12±0.20	13.0
Ligand (3h)	0.26±0.2	3.78±0.1	14.53
Galantamine	2.41±0.10	17.30±0.1	7.17
Rivastigmine	3.01 ± 0.2	0.30±0.1	0.10

Interaction of Copper Complexes with Microorganisms

Due to the redox mechanisms involved in their biological activity, copper complexes are physiologically active. Different microorganisms (1 mM final concentration) were combined in culture media with [Cu-g(OAc)(H_2O)] in DMSO and their UV–Vis spectra were collected at various stages throughout incubation. After interacting with the diverse microorganisms, the band of [Cu-g(OAc)(H_2O)] complex in the culture media at about 410 nm vanished. It's worth noting that the [Cu-g(OAc)(H_2O)] complex has a band at 332 nm, indicating that the complex underwent a first transformation right away (shift to 410 nm), followed by a second transformation after 24 hrs. The loss of the Cu(I) complex's distinctive band at 332 nm suggests that a redox event occurred.

Differences in cell wall and/or membrane structure could explain the observed heterogeneity in copper complex activity across the many classes of species investigated (gram-positive bacteria; peptidoglycan and teichoic acid; gram-negative bacteria; peptidoglycan and liposaccharide). The inclusion of the lipophilic group C=N and the more extensive hetero aromatic ring system of antipyrinyl are likely to impart increased lipophilicity on [Cu-L(OAc)(H_2O)], allowing it to breach the cell wall and induce detrimental intracellular interactions. [Cu-g(OAc)(H_2O)] (MIC = 6 μg/ml) complex was shown to have good antifungal activity against *C. albicans* among the compounds examined. We believe this result is critical since it is extremely hazardous to humans.

Conclusion

The demand for chemically modulated natural products with various pharmacophores for anticancer applications is increasing. The goal of this research was to use the Mannich base technique to design and produce chrysin derivatives. They were structurally elucidated by UV, FT-IR, NMR, Mass and CHN. Four compounds, Cu-e, Cu-f, Cu-g and Cu-h were of great interest

as they exhibited potent free radical scavenging ability by DPPH and SOD mimics. The DNA binding results showed that the complexes can bind to DNA through intercalation mode. Treatment with the copper complexes invariably increased the CAT activity and reduced the stress in liver cells. Together present results point to the anti-inflammatory properties of the chrysin derivative of copper complexes, especially compounds Cu-g and Cu-h, which showed the potential and anti-inflammatory properties and supports future evaluation of bioactive compounds towards therapeutics, tuberculosis (copper complex Cu-g) in cell-based and/or in animal experimental assay methods. They were screened for *in vitro* anticancer efficiency against human cell lines namely MCF-7 and HeLa. The synthesized ligand exhibited selective inhibition (AChE & BuChE), IC_{50} values higher than as compared to standard, Rivastigmine and Galantamine. The synthesized Cu(II) complex displayed an effective inhibition activity of α-glucosidase compared to the standard inhibitor (DNJ) and may be significant in future for antidiabetic and other related disorders. Among the synthesized compounds, Cu-g showed higher anticancer potency as compared with those of other copper complexes and standard. These findings imply that the furan ring is important for antimicrobial and anticancer activity and that it can be used to boost antimicrobial and anticancer efficacy in chrysin derivatives of copper complexes by undergoing chemical transformations. The improved anti-proliferative efficiencies were linked to free hydroxyl groups and B-ring nitrogen substituent, according to the chemical structural core-biological efficiency association. Following clinical studies, these chrysin scaffolds can be used as a skeleton for the synthesis of heterocycle-containing chrysin derivatives with potential anticancer medicines.

Abbreviations

MIC: Minimum inhibitory concentration; DPPH: 2,2-diphenyl-1-picrylhydrazyl; NBT: Nitrobluetetrazolium; SOD: Superoxide dismutase; CT: Calf-thymus; EB: Ethidium bromide; K_{sv}: Stern-Volmer quenching constant; $K_{q:}$ Quenching constant; K_{bin}: Binding constant; HeLa: Human cervical cancer cells; HCT116: Colon cancer cells; MTT: (3-(4,5-dimethylthiazol-2-yl)-2,5-diphenyl-tetrazolium bromide); IC_{50}: Half maximal inhibitory concentration: CAT: Catalase activity; ChEIs: Cholinesterase inhibitors.

Declarations

Acknowledgments

We thank the Head, Department of pharmaceutical chemistry, Manonmaniam Sundaranar University for providing the necessary facilities.

Author contributions

Ebenezer Bonpandi: Formal Analysis; Methogology. Investigation, **Nagashri Kandasamy:** Resources; Supervision.

Funding

The author(s) reported there is no funding associated with the work featured in this article.

Availability of data and material

The authors confirm that the data supporting the findings of this study are available within the article and its supplementary materials.

Ethics approval and concept to participate

Not applicable

Consent for publication

Not applicable

Competing of interest

The authors declare that they have no competing of interest.

Publisher's note Springer Nature remains neutral with regard to jurisdictional claims in published maps and institutional affiliations.

Author details

[1]Department of Pharmaceutical Chemistry, Manonmaniam Sundaranar University, Tirunelveli 627012, Tamilnadu, India.
[2]Department of Chemistry, Manonmaniam Sundaranar University, Tirunelveli-627012, Tamilnadu, India.

References

1. K. Suresh Babu; T. Hari Babu; P.V. Srinivas; K. Hara Kishore; U.S.N. Murthy; J. Madhusudana Rao (2006). Synthesis and biological evaluation of novel C (7) modified chrysin analogues as antibacterial agents. , 16(1), 221–224. doi:10.1016/j.bmcl.2005.09.009.
2. Anari, Elham; Akbarzadeh, Abolfazl; Zarghami, Nosratollah (2015). Chrysin-loaded PLGA-PEG nanoparticles designed for enhanced effect on the breast cancer cell line. Artificial Cells, Nanomedicine, and Biotechnology, 44(6), 1410-1416. doi:10.3109/21691401.2015.1029633.
3. Janusz Pusz; Bronisława Nitka; Agnieszka Zielińska; Iwona Wawer (2000). Synthesis and physicochemical properties of the Al(III), Ga(III) and In(III) complexes with chrysin. , 65(3), 245–253. doi:10.1016/s0026-265x(00)00121-1.
4. Munoz, Vanesa A.; Ferrari, Gabriela V.; Sancho, Matias I.; Montaña, Maria P. (2016). Spectroscopic and Thermodynamic Study of Chrysin and Quercetin Complexes with Cu(II). Journal of Chemical & Engineering Data, 61(6), 987-995. doi:10.1021/acs.jced.5b00837.
5. Bent H Havsteen (2002). The biochemistry and medical significance of the flavonoids. , 96(2-3), 67–202. doi:10.1016/s0163-7258(02)00298-x.
6. Catherine A. Rice-Evans; Nicholas J. Miller; George Paganga (1996). Structure-antioxidant activity relationships of flavonoids and phenolic acids. , 20(7), 933–956. doi:10.1016/0891-5849(95)02227-9.
7. J.P. Cornard; L. Dangleterre; C. Lapouge (2006). DFT and TD-DFT investigation and spectroscopic characterization of the molecular and electronic structure of the Zn(II)–3-hydroxyflavone complex. , 419(1-3), 304–308. doi:10.1016/j.cplett.2005.11.101.
8. LUO, X., YU, X., LIU, S., DENG, Q., LIU, X., PENG, S., CAO, Y. (2015). The role of targeting kinase activity by natural products in cancer chemoprevention and chemotherapy (Review). Oncology Reports, 34(2), 547–554. doi:10.3892/or.2015.4029.
9. Cao, Y., DePinho, R. A., Ernst, M., & Vousden, K. (2011). Cancer research: past, present and future. Nature Reviews Cancer, 11(10), 749–754. doi:10.1038/nrc3138.
10. Ding, Y. et al. (2017). Flavonoids from persimmon (Diospyros kaki L.) leaves inhibit proliferation and induce apoptosis in PC-3 cells by activation of oxidative stress and mitochondrial apoptosis. Chemico-biological interactions 275, 210–217. doi.org/10.1016/j. cbi.2017.07.026.
11. Dai, J., Van Wie, P. G., Fai, L. Y., Kim, D., Wang, L., Poyil, P., … Zhang, Z. (2016). Downregulation of NEDD9 by apigenin suppresses migration, invasion, and metastasis of colorectal cancer cells. Toxicology and Applied Pharmacology, 311, 106–112. doi:10.1016/j.taap.2016.09.016.
12. Kim, E. J., Kwon, K. J., Park, J.-Y., Lee, S. H., Moon, C.-H., & Baik, E. J. (2002). Effects of peroxisome proliferator-activated receptor agonists on LPS-induced neuronal death in mixed cortical neurons: associated with iNOS and COX-2. Brain Research, 941(1-2), 1–10. doi:10.1016/s0006-8993(02)02480-0.
13. Matsuo, N., Yamada, K., Yamashita, K., Shoji, K., Mori, M., & Sugano, M. (1996). Inhibitory effect of tea polyphenols on histamine and leukotriene B4 release from rat peritoneal exudate cells. In Vitro Cellular & Developmental Biology - Animal, 32(6), 340–344. doi:10.1007/bf02722960.

14. MIURA, S., WATANABE, J., SANO, M., TOMITA, T., OSAWA, T., HARA, Y., & TOMITA, I. (1995). Effects of Various Natural Antioxidants on the Cu2+-Mediated Oxidative Modification of Low Density Lipoprotein. Biological & Pharmaceutical Bulletin, 18(1), 1–4. doi:10.1248/bpb.18.1.
15. Veselovskaya, M. V., Garazd, M. M., Ogorodniichuk, A. S., Garazd, Y. L., & Khilya, V. P. (2008). Synthesis of amino-acid derivatives of chrysin. Chemistry of Natural Compounds, 44(6), 704–711. doi:10.1007/s10600-009-9194-4.
16. Fonseca, S. F., Lima, D. B., Alves, D., Jacob, R. G., Perin, G., Lenardão, E. J., & Savegnago, L. (2015). Synthesis, characterization and antioxidant activity of organoselenium and organotellurium compound derivatives of chrysin. New Journal of Chemistry, 39(4), 3043–3050. doi:10.1039/c4nj02329c.
17. Shabbir, M., Akhter, Z., Ahmad, I., Ahmed, S., McKee, V., Ismail, H., & Mirza, B. (2017). Copper (II) complexes bearing ether based ON donor bidentate Schiff bases: Synthesis, characterization, biological and electrochemical investigations. Polyhedron, 124, 117–124. doi:10.1016/j.poly.2016.12.039.
18. Santini, C., Pellei, M., Gandin, V., Porchia, M., Tisato, F., & Marzano, C. (2013). Advances in Copper Complexes as Anticancer Agents. Chemical Reviews, 114(1), 815–862. doi:10.1021/cr400135x.
19. Ruiz-Azuara, L., & E. Bravo-Gomez, M. (2010). Copper Compounds in Cancer Chemotherapy. Current Medicinal Chemistry, 17(31), 3606–3615. doi:10.2174/092986710793213751.
20. Hu, K., Liu, C., Li, J., & Liang, F. (2018). Copper(II) complexes based on quinoline derived Schiff-base ligands: synthesis, characterization, HSA/DNA binding ability, and anticancer activity. MedChemComm. doi:10.1039/c8md00223a.
21. Kalanur, S. S., Katrahalli, U., & Seetharamappa, J. (2009). Electrochemical studies and spectroscopic investigations on the interaction of an anticancer drug with DNA and their analytical applications. Journal of Electroanalytical Chemistry, 636(1-2), 93–100. doi:10.1016/j.jelechem.2009.09.018.
22. Yin, F., Zhu, J., Hao, J., Cui, J., & Yang, J. (2013). Synthesis, characterization, crystal structure and antitumor activities of a novel demethylcantharidato bridged copper(II) phenanthroline complex. Science China Chemistry, 56(4), 481–489. doi:10.1007/s11426-013-4865-1.
23. Pistia-Brueggeman, G., & Hollingsworth, R. I. (2001). A preparation and screening strategy for glycosidase inhibitors. Tetrahedron, 57(42), 8773–8778. doi:10.1016/s0040-4020(01)00877-8.
24. Sk, U. H., & Bhattacharya, S. (2006). Prevention of cadmium induced lipid peroxidation, depletion of some antioxidative enzymes and glutathione by a series of novel organoselenocyanates. Environmental Toxicology and Pharmacology, 22(3), 298–308. doi:10.1016/j.etap.2006.04.004.
25. Zhen, Q.-X., Ye, B.-H., Zhang, Q.-L., Liu, J.-G., Hong Li, Ji, L.-N., & Wang, L. (1999). Synthesis, characterization and the effect of ligand planarity of [Ru(bpy)2L]2+ on DNA binding affinity. Journal of Inorganic Biochemistry, 76(1), 47–53. doi:10.1016/s0162-0134(99)00107-5.
26. Geary, W. J. (1971). The use of conductivity measurements in organic solvents for the characterisation of coordination compounds. Coordination Chemistry Reviews, 7(1), 81–122. doi:10.1016/s0010-8545(00)80009-0.
27. Alomar, K., Landreau, A., Kempf, M., Khan, M. A., Allain, M., & Bouet, G. (2010). Synthesis, crystal structure, characterization of zinc(II), cadmium(II) complexes with 3-thiophene aldehyde thiosemicarbazone (3TTSCH). Biological activities of 3TTSCH and its complexes. Journal of Inorganic Biochemistry, 104(4), 397–404. doi:10.1016/j.jinorgbio.2009.11.012.
28. Sreeja, P. B., & Kurup, M. R. P. (2005). Synthesis and spectral characterization of ternary complexes of oxovanadium(IV) containing some acid hydrazones and 2,2'-bipyridine. Spectrochimica Acta Part A: Molecular and Biomolecular Spectroscopy, 61(1-2), 331–336. doi:10.1016/j.saa.2004.04.001.
29. Raman, N., Kulandaisamy, A., Thangaraja, C., Manisankar, P., Viswanathan, S., & Vedhi, C. (2004). Synthesis, structural characterisation and electrochemical and antibacterial studies of Schiff base copper complexes. Transition Metal Chemistry, 29(2), 129–135. doi:10.1023/b:tmch.0000019409.50574.0a.
30. Gaballa, A. S., Asker, M. S., Barakat, A. S., & Teleb, S. M. (2007). Synthesis, characterization and biological activity of some platinum(II) complexes with Schiff bases derived from salicylaldehyde, 2-furaldehyde and phenylenediamine. Spectrochimica Acta Part A: Molecular and Biomolecular Spectroscopy, 67(1), 114–121. doi:10.1016/j.saa.2006.06.031.

31. Prakash, B., Kumar, A., Singh, P. P., & Songachan, L. S. (2020). Antimicrobial and antioxidant properties of phytochemicals. Functional and Preservative Properties of Phytochemicals, 1–45. doi:10.1016/b978-0-12-818593-3.00001-4.
32. Berczyński, P., Kładna, A., Bozdağ Dündar, O., Murat, H. N., Sarı, E., Kruk, I., & Aboul-Enein, H. Y. (2020). Preparation and in vitro antioxidant activity of some novel flavone analogues bearing piperazine moiety. Bioorganic Chemistry, 95, 103513. doi:10.1016/j.bioorg.2019.103513.
33. Gupta, A., & Pandey, A. K. (2020). Antibacterial lead compounds and their targets for drug development. Phytochemicals as Lead Compounds for New Drug Discovery, 275–292. doi:10.1016/b978-0-12-817890-4.00018-4.
34. Raja, D. S., Bhuvanesh, N. S. P., & Natarajan, K. (2012). A novel water soluble ligand bridged cobalt(ii) coordination polymer of 2-oxo-1,2-dihydroquinoline-3-carbaldehyde (isonicotinic) hydrazone: evaluation of the DNA binding, protein interaction, radical scavenging and anticancer activity. Dalton Transactions, 41(15), 4365. doi:10.1039/c2dt12274j.
35. Selvakumaran, N., Bhuvanesh, N. S. P., & Karvembu, R. (2014). Self-assembled Cu(ii) and Ni(ii) metallamacrocycles formed from 3,3,3',3'-tetrabenzyl-1,1'-aroylbis(thiourea) ligands: DNA and protein binding studies, and cytotoxicity of trinuclear complexes. Dalton Trans., 43(43), 16395–16410. doi:10.1039/c4dt01859a.
36. Macías, B., García, I., Villa, M. V., Borrás, J., Castiñeiras, A., & Sanz, F. (2002). Synthesis and characterization of sulfonamides containing 8-aminoquinoline and their Ni(II) complexes. Crystalline structures of the Ni complexes. Polyhedron, 21(12-13), 1229–1234. doi:10.1016/s0277-5387(02)00997-x.
37. Vijayan, P., Viswanathamurthi, P., Sugumar, P., Ponnuswamy, M. N., Balakumaran, M. D., Kalaichelvan, P. T., Butcher, R. J. (2015). Unprecedented formation of organo-ruthenium(ii) complexes containing 2-hydroxy-1-naphthaldehyde S-benzyldithiocarbazate: synthesis, X-ray crystal structure, DFT study and their biological activities in vitro. Inorganic Chemistry Frontiers, 2(7), 620–639. doi:10.1039/c5qi00029g.
38. Yajko, D. M., Madej, J. J., Lancaster, M. V., Sanders, C. A., Cawthon, V. L., Gee, B., & Hadley, W. K. (1995). Colorimetric method for determining MICs of antimicrobial agents for Mycobacterium tuberculosis. Journal of clinical microbiology, 33(9), 2324-2327. doi.org/10.1128/jcm.33.9.2324-2327.1995.
39. Allen, R. G., & Balin, A. K. (1989). Oxidative influence on development and differentiation: An overview of a free radical theory of development. Free Radical Biology and Medicine, 6(6), 631–661. doi:10.1016/0891-5849(89)90071-3.
40. Chaisiriwong, L., Wanitphakdeedecha, R., Sitthinamsuwan, P., Sampattavanich, S., Chatsiricharoenkul, S., Manuskiatti, W., & Panich, U. (2016). A Case-Control Study of Involvement of Oxidative DNA Damage and Alteration of Antioxidant Defense System in Patients with Basal Cell Carcinoma: Modulation by Tumor Removal. Oxidative Medicine and Cellular Longevity, 2016, 1–12. doi:10.1155/2016/5934024.

Schemes

Scheme 1 & 2 are available in Supplementary Files section.

Figures

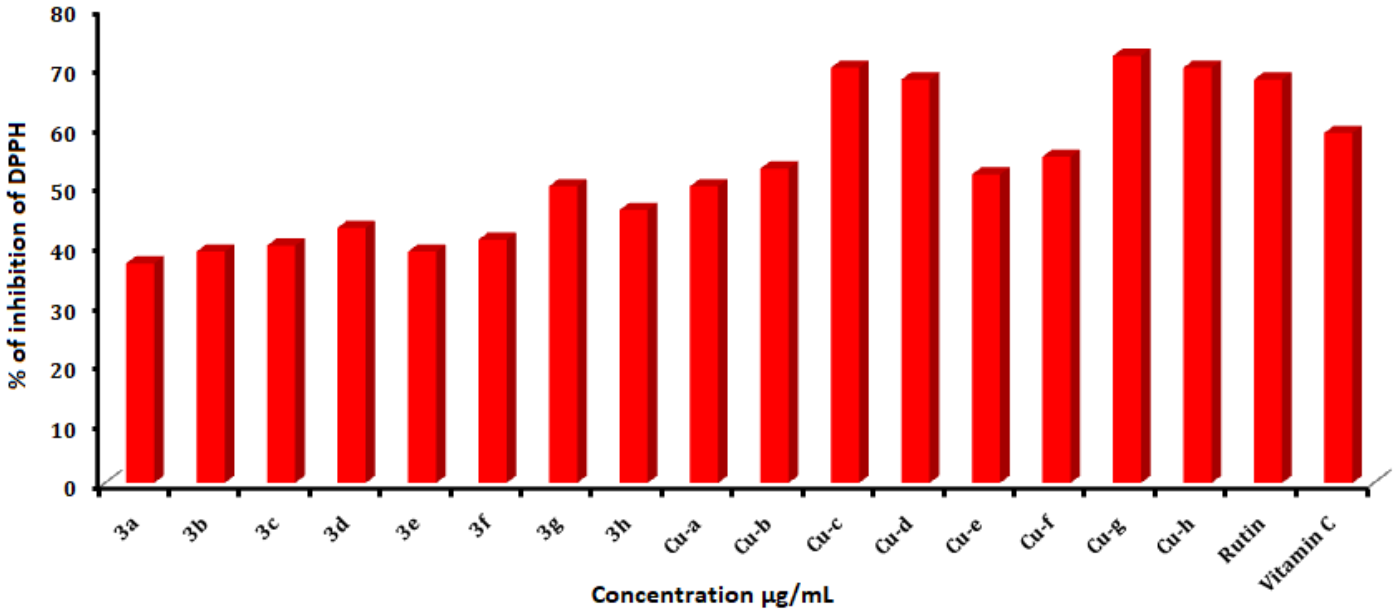


Figure 1

Antioxidant study of ligand and copper complexes.

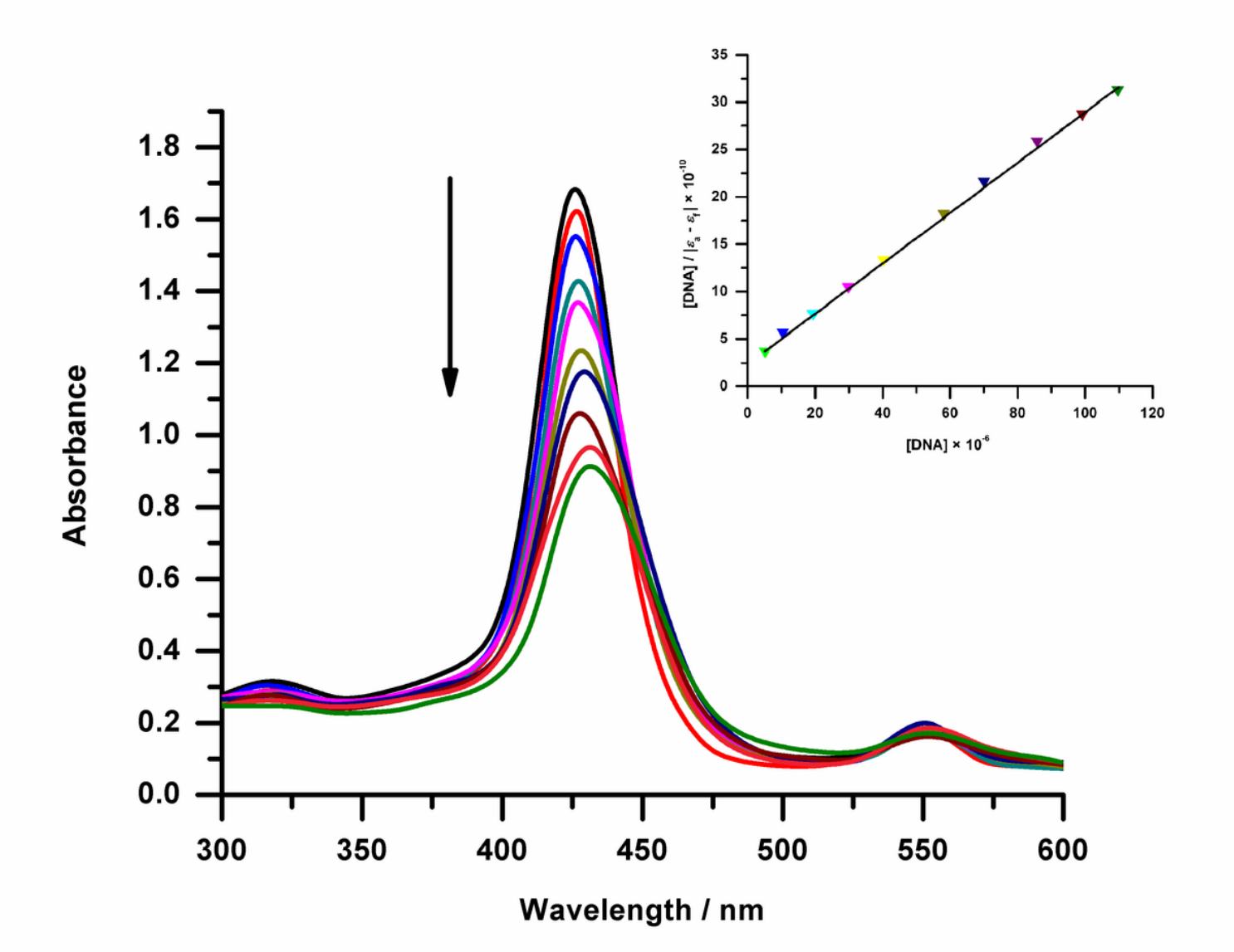


Figure 3

Absorption spectra of 2 in buffer at 25 °C with increasing amounts of CT-DNA. [Copper complex] = 10 μM. Blank arrow indicates the change in absorbance upon increasing the DNA concentration. Inset: Plot of [DNA] vs [DNA] / | $_{b}$- $_{f}$ |.

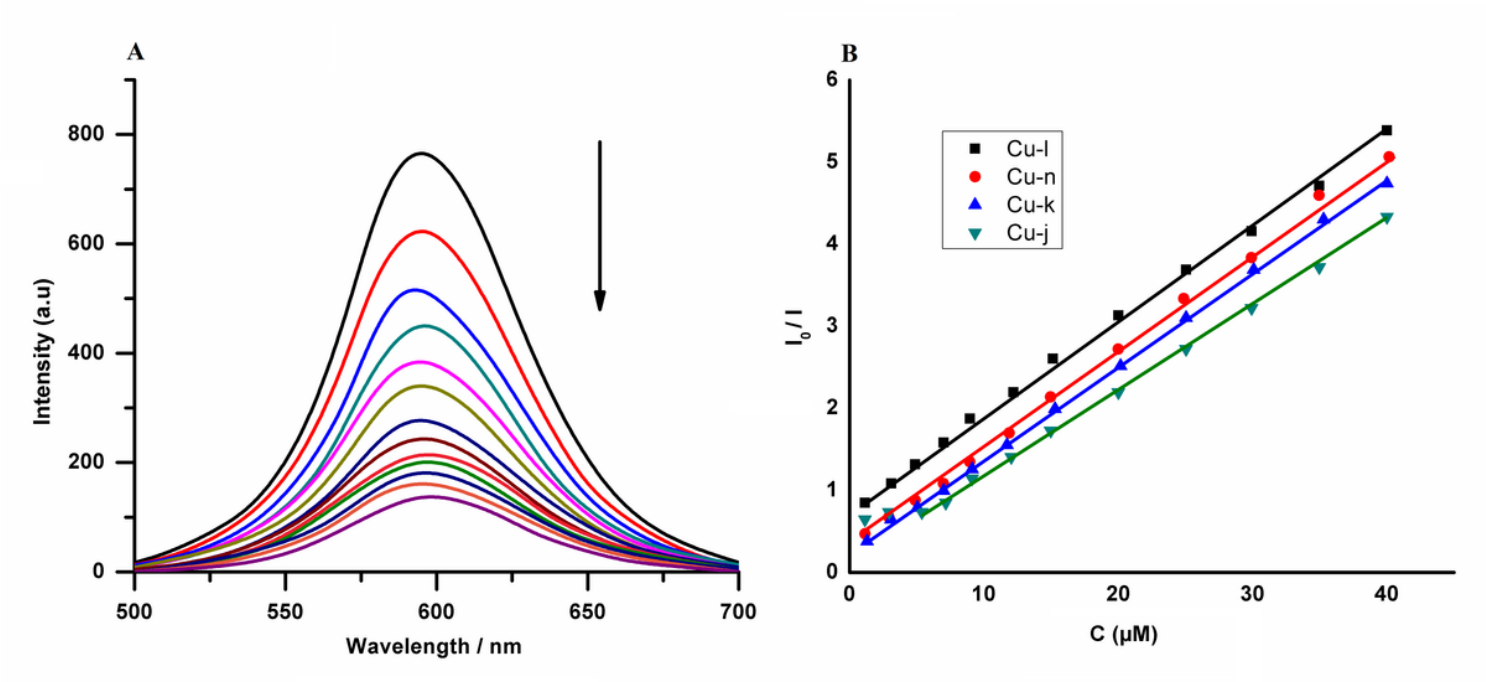


Figure 4

(A) Emission spectra of EtBr (black dotted line), EtBr bound to the CT-DNA (Red line) and addition of with increasing amounts 0–40 μM (other colored lines). [EtBr] =10 μM, [DNA] =10 μM. Arrow indicates changes of emission intensity upon increasing the copper complex concentration. (B) Stern-Volmer plots of the EtBr-DNA fluorescence titration for tested copper complexes.

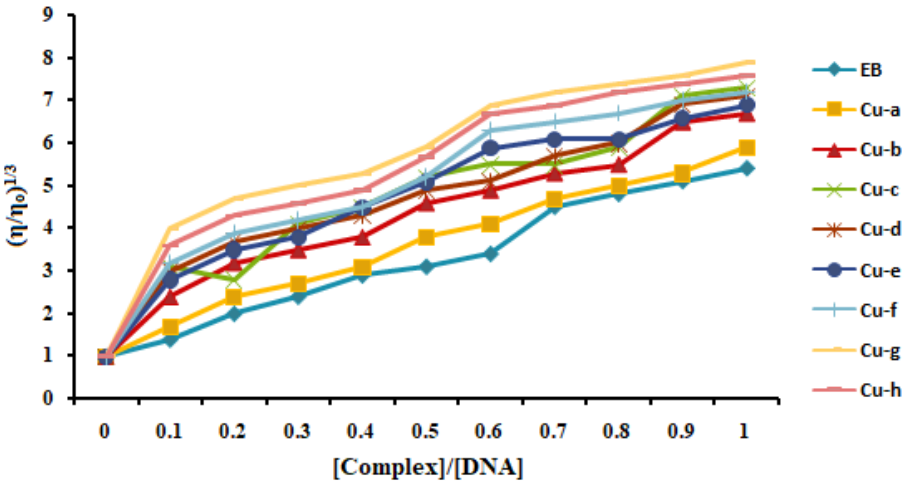


Figure 5

Effect copper complexes on the relative viscosity of CT-DNA (pH = 7.4). Acetonitrile as solvent: [DNA] = 10 μM; 30 ^{o}C; [Complex] = 10 μM.$(\eta/\eta_o)^{1/3}$.

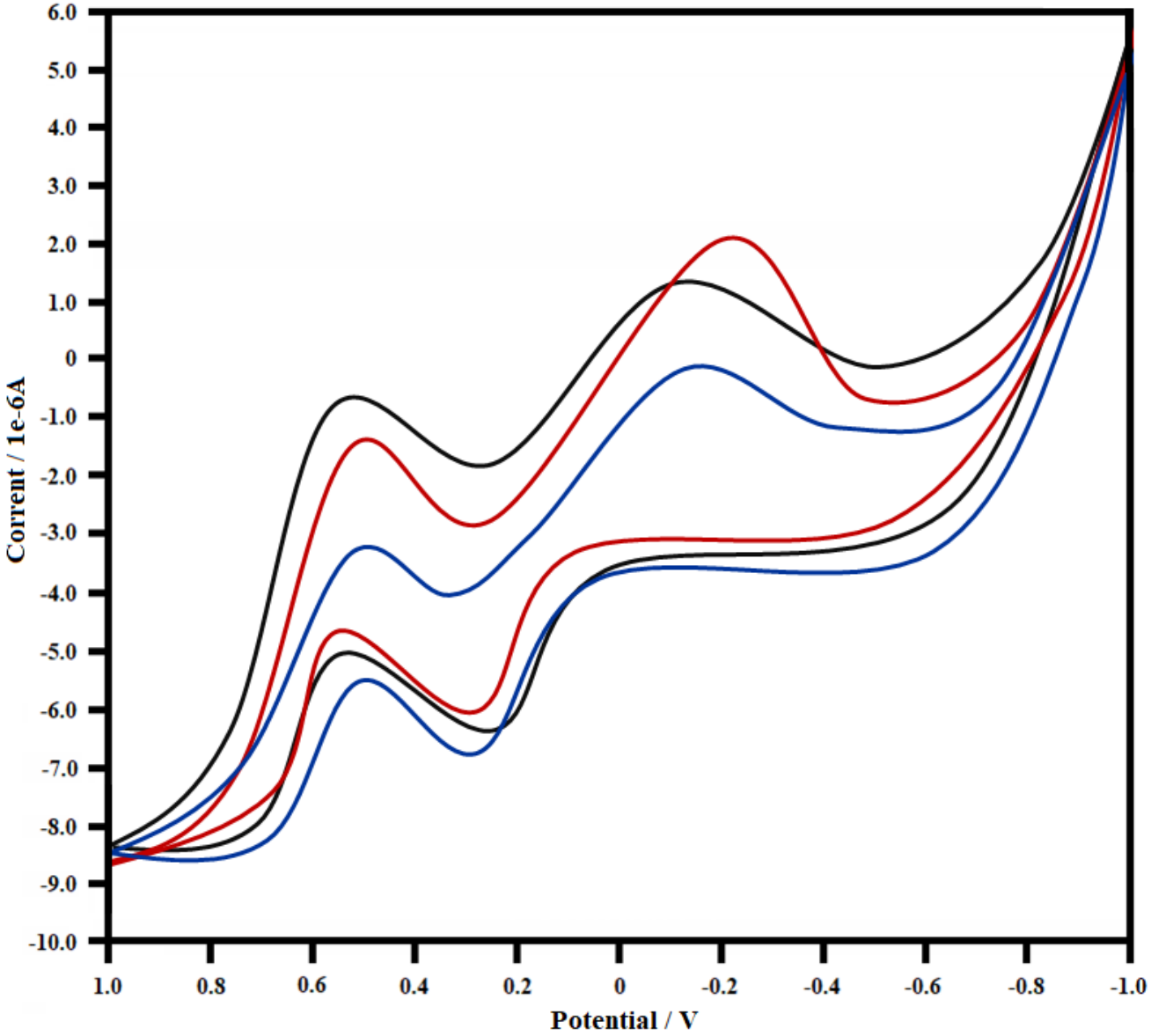


Figure 6

Cyclic voltammetric behaviour of copper complex in the presence and absence of DNA.

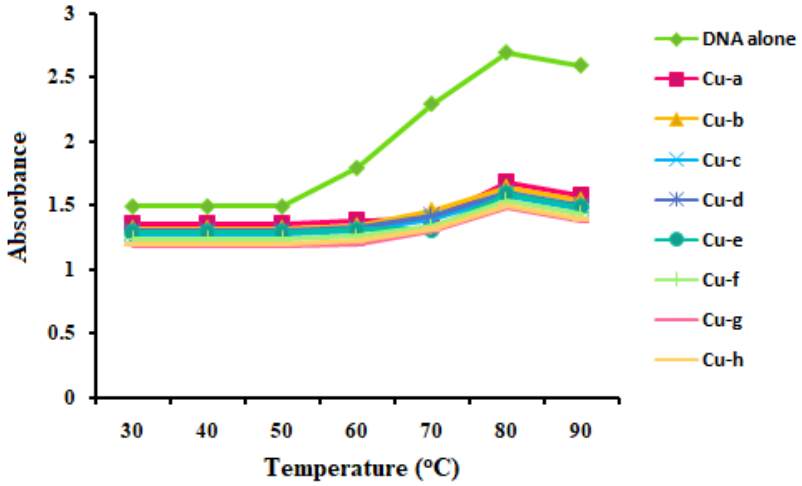


Figure 7

Plots of absorbance versus temperature (^{o}C) for the melting of CT-DNA in the presence and absence of copper complexes. [DNA] = 10 μM; [Complex] = 10 μM.

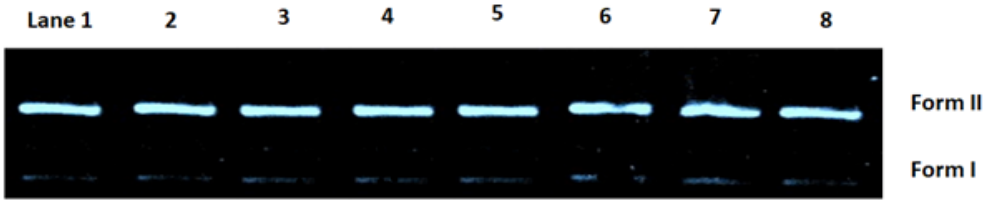


Figure 8

Gel electrophoresis showing the DNA cleavage of the pUC19 DNA incubated at 37 ^{0}C 1 h at a concentration of 50 μM of complex **1–8 (Cu-a, Cu-b, Cu-c, Cu-d, Cu-e, Cu-f, Cu-g** and **Cu-h)** in the presence of H_2O_2 (60 μM) as a co-oxidant: lane 1: pUC19 DNA + H_2O_2 +complex 1 lane 2: pUC19 DNA + H_2O_2 + complex 2 lane 3: pUC19 DNA + H_2O_2 + complex 3 lane 4: pUC19 DNA + H_2O_2 + complex 4 lane 5: pUC19 DNA + H_2O_2 + complex 5 : pUC19 DNA + H_2O_2 + complex 6 : pUC19 DNA + H_2O_2 + complex 7 : pUC19 DNA + H_2O_2 + complex 8.

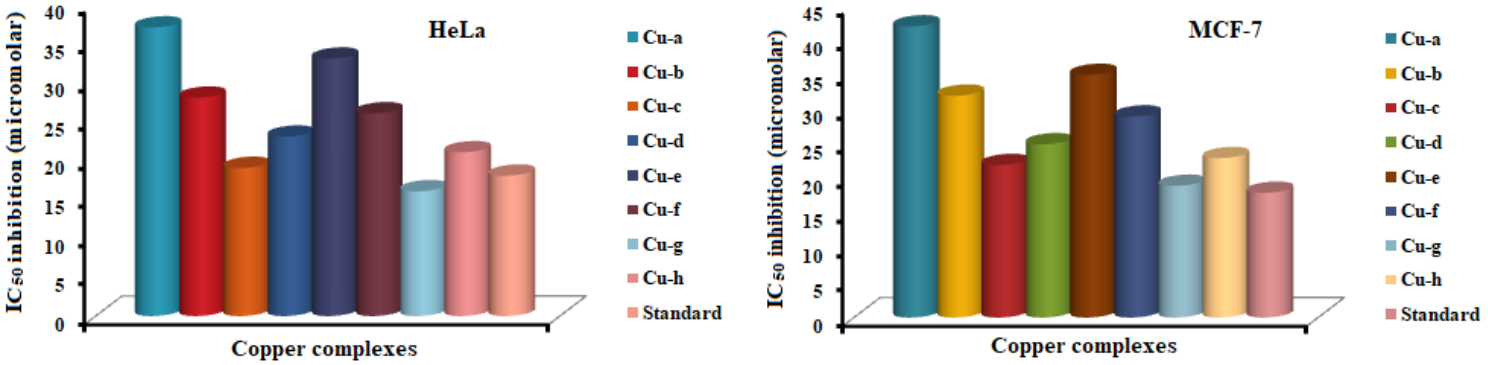


Figure 9

IC_{50} inhibition based on concentration (HeLa and MCF-7) values for chrysin derivatives of copper complexes (Cu-a to Cu-h).

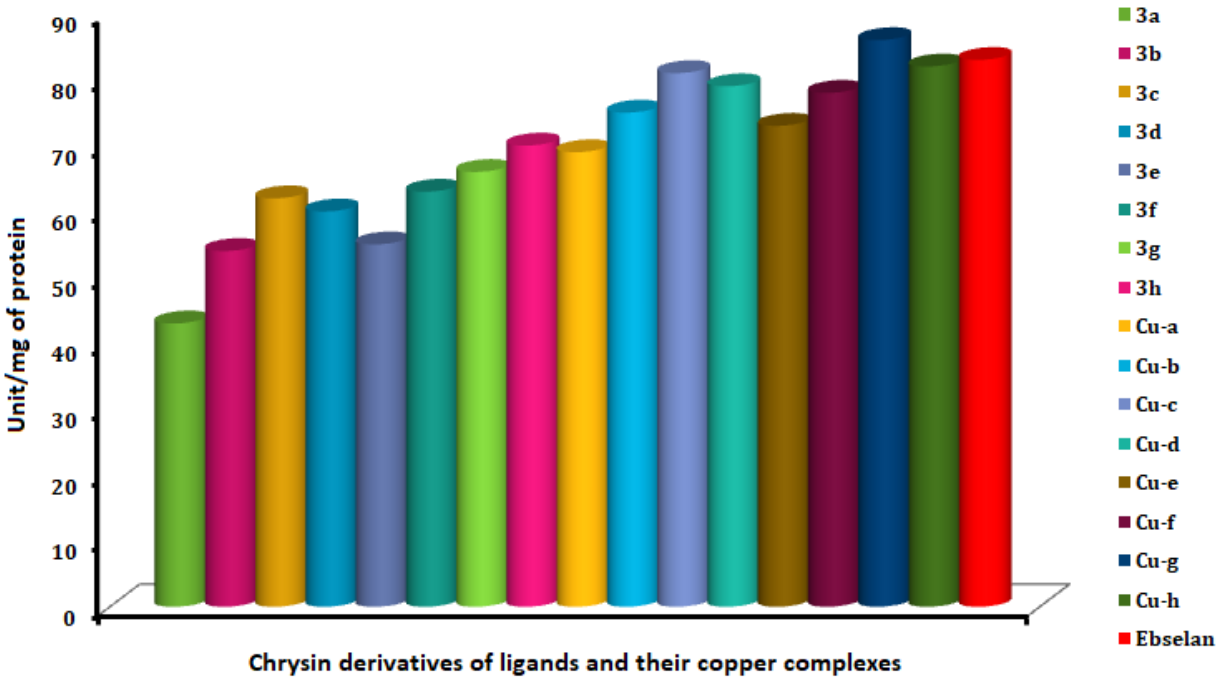


Figure 10

CAT activities of ligands and its copper complexes.

Supplementary Files

This is a list of supplementary files associated with this preprint. Click to download.

- Scheme1.png
- Scheme2.png
- Graphicalabstract.png
- SupplementaryFiles.pdf